

UCLA

UCLA Previously Published Works

Title

Mechanisms of ventricular arrhythmias: from molecular fluctuations to electrical turbulence.

Permalink

<https://escholarship.org/uc/item/1914n3zn>

Journal

Annual review of physiology, 77(1)

ISSN

0066-4278

Authors

Qu, Zhilin
Weiss, James N

Publication Date

2015

DOI

10.1146/annurev-physiol-021014-071622

Peer reviewed

Mechanisms of Ventricular Arrhythmias: From Molecular Fluctuations to Electrical Turbulence

Zhilin Qu¹ and James N. Weiss^{1,2}

Departments of ¹Medicine (Cardiology) and ²Physiology, David Geffen School of Medicine, University of California, Los Angeles, California 90095; email: zqu@mednet.ucla.edu

Annu. Rev. Physiol. 2015. 77:29–55

First published online as a Review in Advance on October 17, 2014

The *Annual Review of Physiology* is online at physiol.annualreviews.org

This article's doi:
10.1146/annurev-physiol-021014-071622

Copyright © 2015 by Annual Reviews.
All rights reserved

Keywords

ventricular arrhythmias, sudden cardiac death, multiscale dynamics, nonlinear dynamics, chaos

Abstract

Ventricular arrhythmias have complex causes and mechanisms. Despite extensive investigation involving many clinical, experimental, and computational studies, effective biological therapeutics are still very limited. In this article, we review our current understanding of the mechanisms of ventricular arrhythmias by summarizing the state of knowledge spanning from the molecular scale to electrical wave behavior at the tissue and organ scales and how the complex nonlinear interactions integrate into the dynamics of arrhythmias in the heart. We discuss the challenges that we face in synthesizing these dynamics to develop safe and effective novel therapeutic approaches.

1. INTRODUCTION

Cardiac arrhythmias have been recognized as a key complication of heart diseases for centuries (1, 2). Generally defined, cardiac arrhythmias refer to conditions in which the electrical activity of the heart becomes too slow, too fast, and/or too irregular. Slow heart rhythms can be readily treated with electronic pacemakers, but rapid heart rhythms that culminate in atrial fibrillation or ventricular fibrillation (VF), in which the electrical activity in the atria or ventricles becomes turbulent, remain leading causes of morbidity and mortality, including sudden cardiac death, particularly in industrialized countries (3). From the first demonstration of electrical activity of the heart in 1856 (1) to today's modern technologies unraveling the genetic basis of many cardiac arrhythmias (4, 5), this problem has been a major focus of medicine for more than a century. However, successful pharmacological treatment is still problematic. Current antiarrhythmic drugs have limited effectiveness, and many can have unintended proarrhythmic effects (6, 7). The most effective treatment for VF is an implantable cardioverter defibrillator (ICD), which can promptly and effectively terminate life-threatening arrhythmias. However, 80% of patients who will die suddenly each year in the United States do not meet current clinical criteria for prophylactic implantation of an ICD (8); moreover, even among those who do meet such criteria, only one in five ICDs will deliver a life-saving shock because of the difficulty in identifying those at highest risk (9). Additionally, ICD treatment is expensive and has significant morbidity.

The limited effectiveness of biologically based antiarrhythmic therapies, as opposed to bioengineering-based strategies, is related to the ubiquitous problem in biomedicine that the relevant biological targets for drug or gene therapy exist at the molecular scale, whereas the arrhythmias exist at the organ scale. Predicting how the behavior of a molecule will affect the properties of the organ is very complex because at each more integrated level, from molecule to molecular signaling complex to organelle to cell to tissue to organ to organism, qualitatively new properties emerge from the complex nonlinear interactions between properties at that level of integration and properties at the next-higher level of integration. In other words, the heart, as is any other organ in the body, is regulated at multiple spatial and temporal scales, and each scale has its own dynamics that then give rise to the dynamics at the next scale.

In this review article, we summarize our current understanding of ventricular arrhythmias, focusing on the multiscale and complex dynamic nature of the problem. After a brief summary of the multiscale dynamics in the heart, we then deconstruct the excitation dynamics in the reverse order: tissue-scale electrical wave dynamics, cellular-scale action potential dynamics, and subcellular- and molecular-scale dynamics. The goal is to illustrate, in a stepwise fashion, how the higher-scale dynamics emerge from lower-scale dynamics. We discuss the challenges and the potential for nonlinear dynamics, combined with new systems approaches, to lead to the development of robust and effective therapeutics. The article involves some important concepts of nonlinear dynamics relevant to arrhythmias (10), such as dynamic instabilities, bifurcation, chaos, synchronization, criticality, and basins of attraction. To help the readers who are not familiar with these concepts, they are explained in more detail in the **Supplemental Text** (follow the **Supplemental Material link** from the Annual Reviews home page at <http://www.annualreviews.org>).

2. MULTISCALE DYNAMICS IN THE HEART

The dynamics of excitation and contraction at different scales in the heart have distinct features. At the molecular scale, dynamics is governed mainly by thermodynamic fluctuations. For instance, ion channels open and close randomly (**Figure 1a**), and thousands of ion channels and ion transporters are distributed in the cell membrane to generate ionic currents for the action potential (**Figure 1b**).

The channels and transporters are typically organized into molecular signaling complexes regulating their activity. In addition to the surface plasma membrane, these molecular signaling complexes often form clusters in intracellular organelles, such as the sarcoplasmic reticulum (SR) and mitochondria. These ion channel clusters open and close collectively to result in organelle-scale dynamics, such as calcium (Ca^{2+}) sparks and mitochondrial flickers (11). For example, a Ca^{2+} spark (**Figure 1c**) is a Ca^{2+} release event of a Ca^{2+} release unit due to the collective opening of the ryanodine receptors (RyRs) triggered by the opening of the associated L-type Ca^{2+} channel cluster or by high intracellular Ca^{2+} . Under normal conditions, the L-type Ca^{2+} channel-triggered Ca^{2+} sparks integrate to give rise to the whole-cell Ca^{2+} transient (**Figure 1b**). Under diseased conditions and/or high intracellular Ca^{2+} load, the Ca^{2+} sparks organize to form different types

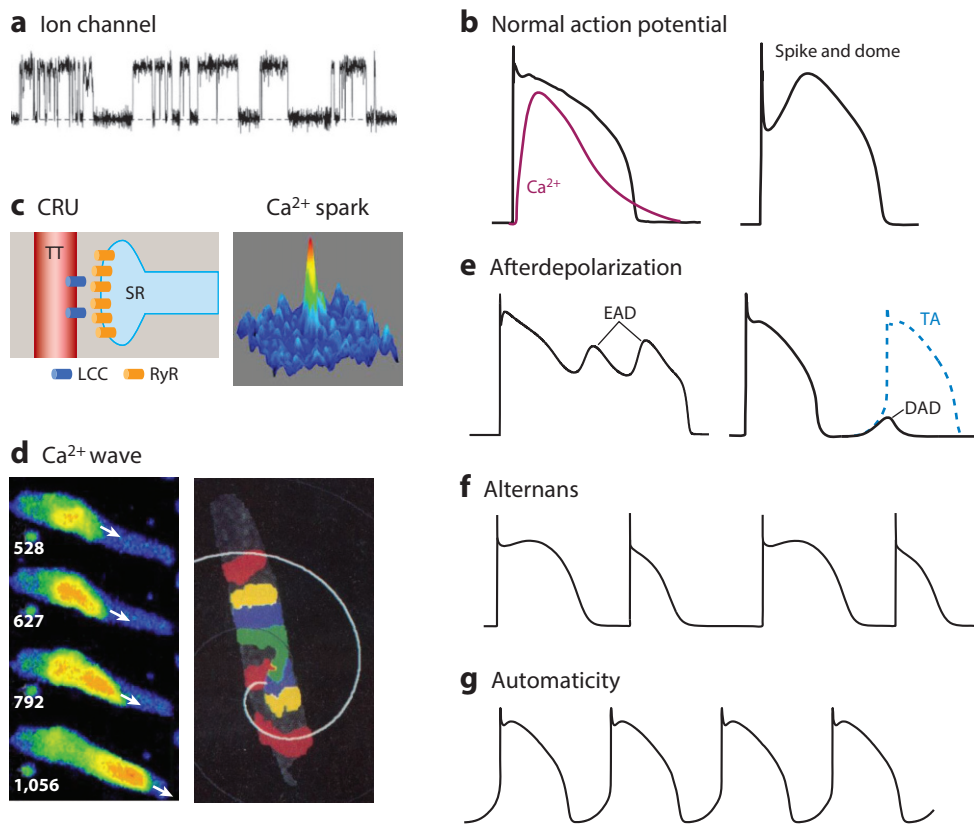


Figure 1

Subcellular and cellular dynamics of ventricular myocytes. (a) A single ion channel opening and closing stochastically. (b) Normal action potentials and Ca^{2+} transient for endocardial myocytes (left) and epicardial myocytes (right). A spike-and-dome morphology occurs in epicardial myocytes. (c) A Ca^{2+} release unit (CRU) that is composed of a ryanodine receptor (RyR) cluster in the sarcoplasmic reticulum (SR) membrane and an L-type Ca^{2+} channel (LCC) cluster in the apposing T-tubule (TT) membrane (left) and a Ca^{2+} spark (right). The spark image was downloaded from <https://sites.google.com/site/sparkmasterhome/faq>. (d) A planar Ca^{2+} wave (left; arrows indicate the direction of propagation, and the numbers indicate time in milliseconds) from a Purkinje cell (from Reference 150 with permission) and a spiral Ca^{2+} wave (right) (from Reference 151 with permission). (e) Early afterdepolarizations (EADs), delayed afterdepolarizations (DADs), and triggered activity (TA). (f) Action potential alternans. (g) Spontaneous oscillations (automaticity).

of intracellular Ca^{2+} waves (**Figure 1d**) to generate whole-cell Ca^{2+} oscillations [the analogy for mitochondria is mitochondrial depolarization waves and oscillations (12)].

At the cellular scale, the subcellular dynamics couple with surface membrane ionic currents to result in various excitation and contraction dynamics. Under normal conditions, a ventricular myocyte is excitable: A normal action potential and a corresponding Ca^{2+} transient triggering contraction are generated in response to a stimulus (**Figure 1b**). The action potential morphology and duration are heterogeneous throughout the heart, with epicardial but not endocardial myocytes tending to exhibit a spike-and-dome morphology (right panel in **Figure 1b**). Under certain diseased conditions when outward currents are reduced and/or inward currents are increased, voltage depolarizations (oscillations) can occur during the repolarization phase of the action potential, termed early afterdepolarizations (EADs) (**Figure 1e**). During the diastolic phase, a spontaneous Ca^{2+} wave elevates intracellular Ca^{2+} , which increases the Na^+ - Ca^{2+} exchange current (I_{NCX}) to cause a voltage depolarization termed a delayed afterdepolarization (DAD) (**Figure 1e**). If the Ca^{2+} transient is large enough to depolarize the voltage to the threshold for Na^+ channel activation, a full action potential occurs, which is termed triggered activity. An EAD, if its takeoff potential is low and amplitude is large, can also cause triggered activity. During rapid pacing, the action potential duration (APD) of a normal ventricular myocyte may exhibit a long-short-long-short pattern termed APD alternans (**Figure 1f**). Under diseased conditions, APD alternans can often occur at much slower heart rates. A ventricular cell can also become oscillatory (**Figure 1g**) due to aberrant ionic current or Ca^{2+} cycling properties, termed automaticity.

At the tissue and organ scales, the cellular dynamics combine with tissue heterogeneities and cell coupling properties to generate the electrical wave dynamics underlying normal sinus rhythm, as well as different types of arrhythmias. During normal sinus rhythm, the impulses originating from the sinoatrial node follow an anatomically defined conduction pathway culminating in synchronous excitation of the ventricles. These excitation waves are termed rectilinear (or planar) waves (**Figure 2a**). Under diseased conditions, different types of electrical waves can occur in the ventricles, resulting in different types of ventricular arrhythmias. The first type of wave is termed a target wave (or focal excitation), in which spontaneous excitation originates from a local region of the ventricles due to heterogeneities in cellular properties and propagates outward to excite other regions of the heart (**Figure 2b**). The second type of wave is an excitation wave propagating around an obstacle, termed anatomical reentry (**Figure 2c**). The third type of wave does not require heterogeneities or an obstacle and can even occur in completely homogeneous tissue; this type is termed a spiral wave (**Figure 2d**) or sometimes a rotor or functional reentry. Because the heart is a three-dimensional object, the spiral wave in two-dimensional tissue is technically a scroll wave in the real heart (**Figure 2e,f**), but here we use spiral wave to refer to both.

The dynamics at a higher scale depend on the dynamics at lower scales, but the information flow is bidirectional so that the dynamics at a lower scale are also modulated by the dynamics at the higher scales. For example, EADs in an action potential are caused by aberrant ion currents and Ca^{2+} cycling properties, but the occurrence of EADs can bring more Ca^{2+} into the cell to potentiate Ca^{2+} waves due to L-type Ca^{2+} channel opening during the EADs. Furthermore, besides the typical Ca^{2+} cycling, action potential, and electrical wave dynamics shown in **Figures 1** and **2**, more complex dynamics can emerge due to heterogeneities and dynamic instabilities. These dynamics at different scales play critical roles in initiating arrhythmias, as well as giving rise to different types of arrhythmias. Therefore, to understand the mechanisms of arrhythmias and to develop molecularly based therapeutics, one needs to understand how molecular behaviors relate to electrical wave dynamics; i.e., one needs to relate the dynamics at each lower scale (in both time and space) to the dynamics at the next higher scale, sequentially from molecule to organism. For

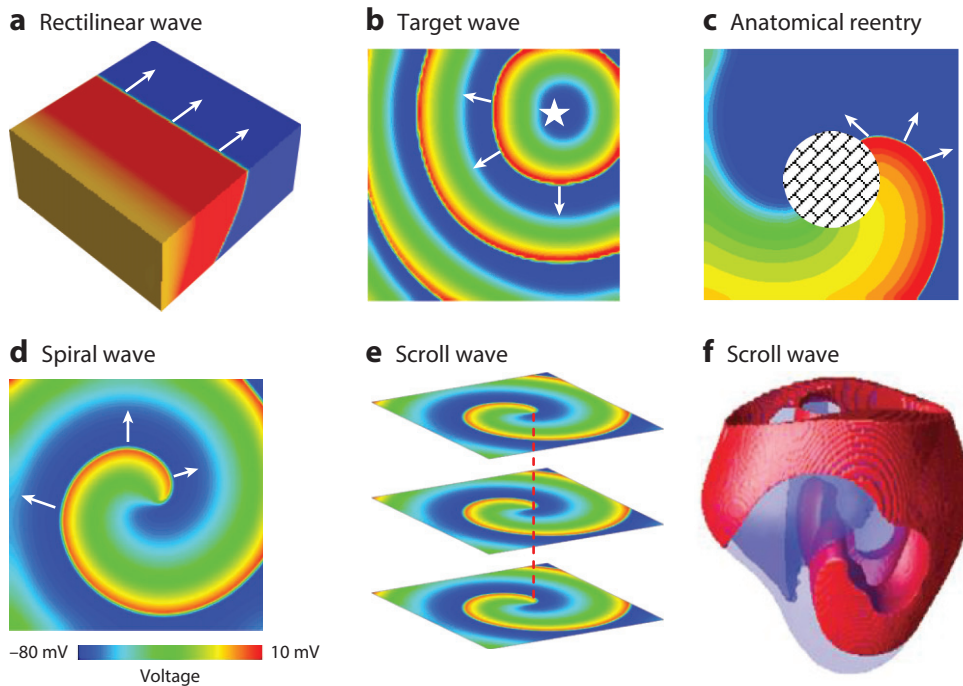


Figure 2

Tissue-scale excitation dynamics. (a) A rectilinear (planar) wave. (b) A focal excitation (target wave). (c) Reentry around an obstacle. (d) A spiral wave. (e) A scroll wave. (f) A scroll wave in the ventricles (from Reference 152 with permission). Voltage levels are indicated by the color bar, and arrows indicate the directions of propagation in panels *a–e*. In panel *f*, only voltage higher than a certain value is colored in red for three-dimensional visualization.

example, to understand how a mutation in RyRs is linked to arrhythmias, one needs to understand, in sequence, the following: how the mutation modifies the opening and closing properties of RyRs; how RyRs in a cluster interact with each other to affect Ca^{2+} spark behavior both normally and when various signaling pathways are activated; how Ca^{2+} sparks organize into Ca^{2+} waves and oscillations; how Ca^{2+} waves and oscillations affect the cellular action potential dynamics, such as alternans, EADs, and DADs; and finally how these cellular action potential dynamics synchronize at the tissue and organ levels to generate the electrical wave dynamics leading to different types of arrhythmias. In the sections below, we summarize our current understanding of the multiscale dynamics in the heart to illuminate first how the dynamics at a higher scale emerge from the dynamics of a lower scale and then how the dynamics at the higher scale feed back to modulate the properties at the lower scale.

3. ARRHYTHMOGENIC ELECTRICAL WAVE DYNAMICS AT THE TISSUE AND ORGAN SCALES

Different electrical wave dynamics at the tissue and organ scales give rise to different types of arrhythmias. These wave dynamics are caused by either preexisting tissue heterogeneities or dynamic instabilities or their interactions, which are summarized in the sections below.

3.1. Focal Excitations Due to Triggered Activity and Automaticity

A focal excitation (**Figure 2b**) is a spontaneous firing of a group of cells in cardiac tissue. Spontaneous firing can be due to either triggered activity or automaticity. Under normal conditions, thousands of cells need to fire synchronously to overcome the strong sink effect of the adjacent unexcited cells, but under conditions of weak gap junction coupling, such as in fibrotic or ischemic tissue, the number of the spontaneously firing cells required to form a focal excitation is substantially reduced (13).

Traditionally, focal excitations have been thought to require heterogeneous tissue, i.e., one region of the tissue exhibiting spontaneous firing that propagates into surrounding quiescent regions. Intuitively, if all cells are identical and therefore spontaneously fire simultaneously in a homogeneous tissue, the whole tissue fires together, and no localized focus can form. However, focal excitations can also occur in homogeneous tissue via self-organizing pattern formation (**Supplemental Figure 1a**). Our recent study (14) showed that when the action potential develops EADs, the dynamics at the cellular level can be chaotic such that at the tissue level, regional chaos synchronization results in the formation of islands of long APD with EADs next to regions with normal APD without EADs, forming a complex spatiotemporal pattern. The EADs propagate out of the islands, forming a pattern of multiple, shifting focal excitations. The foci formed via this mechanism are not stable but vary dynamically in space and time due to the spatiotemporal chaotic dynamics. In contrast, focal excitations purely due to a tissue heterogeneity remain fixed in space. This dynamic feature agrees with the experimental observations of focal arrhythmias in drug-induced long-QT (LQT) syndrome, in which multiple foci arising dynamically from different locations occur in space and time (15, 16). Tissue heterogeneities and random ion channel fluctuations potentiate these dynamics (17, 18). The dynamic mechanisms of multiple foci nicely account for two features of polymorphic ventricular tachycardia (VT): (a) the observation that polymorphic VT can be sustained for long periods in tissue, even though single cells usually exhibit only one or several EAD-triggered action potentials (17), and (b) the frequent spontaneous termination of polymorphic VT, in particular torsade de pointes (19).

A clear example of heterogeneity interacting with dynamics is bidirectional VT in catecholaminergic polymorphic VT (CPVT), in which two focal excitations can perpetuate each other to form a stable reciprocal firing pattern (20). A simulation study by Baher et al. (21) demonstrated this mechanism. Specifically, as the heart rate increases, a focal excitation due to a DAD occurs at a certain location (e.g., the left bundle branch), which propagates reciprocally to the contralateral (right) bundle branch and causes a focal excitation there via the same mechanism. The excitation from the right then propagates to the left and causes another focal excitation in the left branch, and so on in a reciprocating ping-pong fashion.

3.2. Reentry

Two general categories of reentry occur in cardiac tissue: reentry around an obstacle (anatomical reentry; **Figure 2c**), such as reentry using a specialized pathway (e.g., a bypass tract or around a scar), and spiral wave reentry (also known as scroll wave, rotor, or functional reentry; **Figure 2d**). Anatomical reentry was first demonstrated experimentally in an annulus of cardiac tissue by Mines (22) approximately a century ago. In many cases, anatomical reentry is stable, resulting in monomorphic VT. However, depending on the path length of the reentry circuit relative to the wavelength of the impulse, reentry may become unstable, leading to more complex morphologies of arrhythmias, such as polymorphic VT and VF.

Spiral waves are a generic feature of wave dynamics in excitable media that can occur in both homogeneous tissue and heterogeneous tissue. Spiral waves were first demonstrated in chemical

reactions (23) and later in cardiac tissue (24). Spiral waves can be stable, resulting in a periodic behavior manifesting as monomorphic VT, but can also be unstable. In the latter case, the spiral wave meanders and drifts and can spontaneously break up into multiple spiral waves—a turbulent state of electrical waves. A meandering or drifting spiral wave can give rise to polymorphic VT or torsade de pointes, whereas frank breakup along the arm of a spiral wave results in fibrillation due to the generation of new spiral waves and/or fibrillatory conduction block.

Computer modeling as well as experimental studies have shown that the slope of the APD restitution curve is a key parameter that determines the stability of the spiral wave reentry in cardiac tissue such that a spiral wave becomes more unstable as the slope of APD restitution curve becomes steeper (25, 26). APD restitution is defined as the relationship between the APD and its preceding diastolic interval (see **Supplemental Figure 2** for more detailed definition), which is a measure of the state of ion channel recovery from their openings in the previous action potential. When the APD restitution curve is steep enough, there is spiral wave breakup (**Supplemental Figure 1b,d,e**), in which a turbulent electrical state maintained by irregular spiral waves (or wavelets) appears and disappears in a chaotic manner. Spiral breakup as a mechanism of fibrillation agrees with Moe et al.'s (27) original multiple wavelets hypothesis, in which fibrillation is characterized by multiple wandering wavelets in the heart. However, tissue heterogeneities can also promote spiral wave meandering and wave breaks. For example, in a tissue with large refractory gradient, fibrillatory conduction block can occur. In this scenario, a fast spiral wave generates higher-frequency excitations that are unable to propagate 1:1 into surrounding regions with longer refractory periods, resulting in wave breaks generating turbulent wave patterns (**Supplemental Figure 1c**). This mechanism is termed mother-rotor fibrillation (2). Because cardiac tissue is heterogeneous, the dominant mechanism depends on the specific disease conditions, and in some conditions, both mechanisms may work in synergy to generate the electrical turbulence of VF.

 [Supplemental Material](#)

3.3. Biexcitability

Biexcitability is a novel wave conduction behavior demonstrated in recent studies (28–30). In both atrial and ventricular tissue, normal wave conduction is driven mainly by the I_{Na} current (I_{Na}), which mediates the initial rapid upstroke of the action potential. Under certain conditions—such as LQT syndrome, in which prolonged APD and EADs occur due to reduced repolarization reserve—cells can develop two stable resting membrane potentials: one typically at approximately -80 mV and one at approximately -50 mV (31). Under these conditions, bistable wave propagation can occur; i.e., a slow conduction mediated by L-type Ca^{2+} current ($I_{Ca,L}$) from the more depolarized resting potential (at which I_{Na} is mostly inactivated) and a fast conduction mediated by both I_{Na} and $I_{Ca,L}$ from the fully repolarized resting potential occur in the same tissue. This behavior is therefore referred to as biexcitability. Chang et al. (28) demonstrated this behavior by showing, in computer simulations, that in a homogeneous tissue two distinct types of spiral waves can be induced, depending on the method of initiation. In the first type of fast spiral wave (**Supplemental Figure 3a**), voltage recovers close to the resting potential (-80 mV), and both I_{Na} and $I_{Ca,L}$ are activated. In the second type of slow spiral wave (**Supplemental Figure 3b**), however, voltage recovers only to approximately -50 mV. Because I_{Na} is inactivated above -60 mV, only $I_{Ca,L}$ is activated, which results in a slower propagation. Under some conditions, both types of conduction occur interchangeably in the same tissue (**Supplemental Figure 3c**). This behavior was experimentally observed in cultured myocyte monolayers (28, 29) and can be seen in recordings during arrhythmias in LQT syndrome (16, 32). Biexcitability may provide a mechanism for torsade de pointes and may explain why torsade de pointes often spontaneously terminates but sometimes degenerates into VF (28, 29).

3.4. Arrhythmia Initiation: Trigger and Substrate Interactions

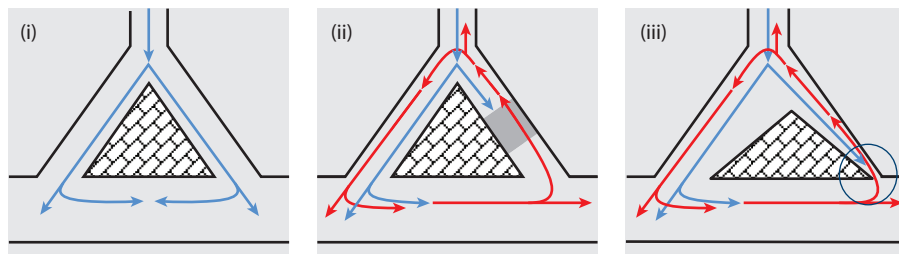
Although understanding reentrant and focal electrical wave behaviors during arrhythmias is important, even more important is understanding how these waves and foci are initiated because from the therapeutic viewpoint, the ideal strategy is to prevent the initiation of arrhythmias. Generally speaking, initiation of reentry requires two factors: a critically timed trigger such as a premature ventricular complex (PVC) and a tissue substrate exhibiting dispersion of refractoriness. On the basis of past studies, we can summarize the most relevant settings as follows.

3.4.1. Induction of arrhythmias around an anatomical obstacle. Reentry around an obstacle can form by different mechanisms (**Figure 3a**). When the tissue around the obstacle is homogeneous and the pathways are wide, a PVC can successfully conduct through both pathways (case *i* in **Figure 3a**) and does not induce reentry. When the tissue around the obstacle is electrically heterogeneous, however, unidirectional conduction block of a properly timed PVC can occur due to dispersion of refractoriness, allowing the antegrade impulse to conduct retrogradely into the blocked pathway, initiating reentry (case *ii* in **Figure 3a**) (22). Another scenario is source-sink mismatch (33, 34), in which one of the pathways has a very narrow exit (case *iii* in **Figure 3a**) and the impulse fails to propagate out of the narrow pathway due to the strong sink effect from the cells outside the exit (i.e., a small number of cells at the exit of the narrow pathway provides the electrical source for a large number of cells outside, and thus the source is weaker than the sink). However, the impulse from the other pathway can enter into the narrow pathway because the source from the outside cells is strong enough (i.e., a large number of cells outside provides the electrical source for a small number of cells in the narrow pathway, and thus the source is stronger than the sink). Because of this source-sink mismatch, reentry can form. This mechanism of reentry initiation can underlie concealed Wolff-Parkinson-White syndrome, a common cause of paroxysmal supraventricular tachycardia, as well as reentry in scarred and fibrotic tissue, such as in the border zone of an infarct.

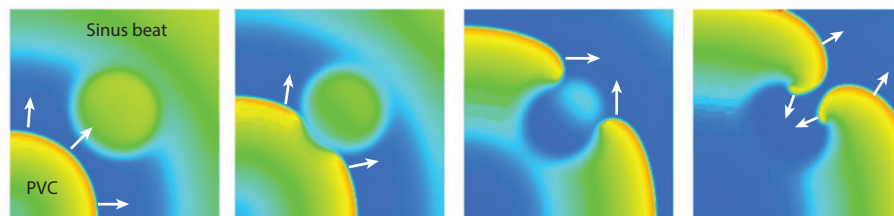
3.4.2. Induction of arrhythmias by a trigger in heterogeneous tissue without anatomic obstacles. In tissue with no obstacles or specialized pathways, unidirectional conduction block can still occur due to dispersion of refractoriness (35). A typical scenario is shown in **Figure 3b**: The central region of the tissue has a longer refractory period so that a PVC originating from a peripheral location may fail to propagate through the central region and propagate around it, reentering from the other side to form so-called figure-of-eight reentry. For reentry to form by this mechanism, the central region needs to be large enough and the PVC timed in a proper window termed the vulnerable window.

3.4.3. Induction of arrhythmias by a trigger and substrate arising from the same process. In the above two mechanisms, the trigger and the substrate emanate from two separate etiologies. In a third mechanism of reentry initiation, both the trigger and the substrate arise from the same cause. For example (**Figure 3c**), if the cells in the central region of a tissue exhibit EADs, but asymmetrical heterogeneities in the tissue alter electrical loading conditions (source-sink mismatch), EADs can propagate outward from one side of the heterogeneous region, but not from the other, leading to initiation of reentry. This scenario has been demonstrated in real cardiac tissue with drug-induced LQT syndrome (32, 36). This same scenario is also responsible for phase 2 reentry (**Supplemental Figure 4**), in which the action potential in the central region exhibits a spike-and-dome morphology (**Figure 1b**) whereas the action potential in the surrounding area exhibits

a Anatomical reentry



b Trigger and substrate from two different sources



c Trigger and substrate from a single source

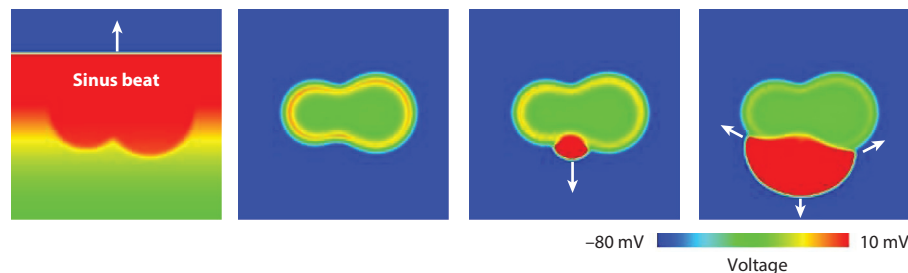


Figure 3

Mechanisms of reentry initiation. (a) Reentry around an anatomic obstacle. (i) Homogeneous refractoriness: A premature ventricular complex (PVC) successfully propagates through both sides of the obstacle without forming reentry. (ii) Heterogeneous refractoriness: The refractory period in one region is longer than elsewhere (e.g., the gray zone in the right pathway) such that a properly timed PVC is blocked in the right pathway, propagates successfully through the contralateral pathway (e.g., the left), and then reenters the right pathway from the retrograde direction, initiating reentry around the obstacle (red arrows). (iii) Narrow pathway: The right pathway has a very narrow exit (indicated by the circle) such that a PVC cannot conduct out of the pathway, but the impulse from outside can enter the pathway, resulting in reentry (red arrows). (b) Reentry in heterogeneous tissue in which the central region has a longer refractory period than the rest of the tissue. (c) Reentry induction by a trigger and substrate from the same source. Cells in the central region exhibit early afterdepolarizations.

early repolarization (short APD) without a dome. Phase 2 reentry initiates reentrant arrhythmias in both acute ischemia and Brugada syndrome (37–39).

3.4.4. Induction of arrhythmias via dynamic instabilities. In the three mechanisms of reentry initiation described above, the heterogeneities can either be preexisting or arise from dynamic instabilities. For example, spatially discordant APD alternans (**Figure 4a**) creates tissue heterogeneity via dynamic instabilities (40, 41), even when all the cells in the tissue have identical

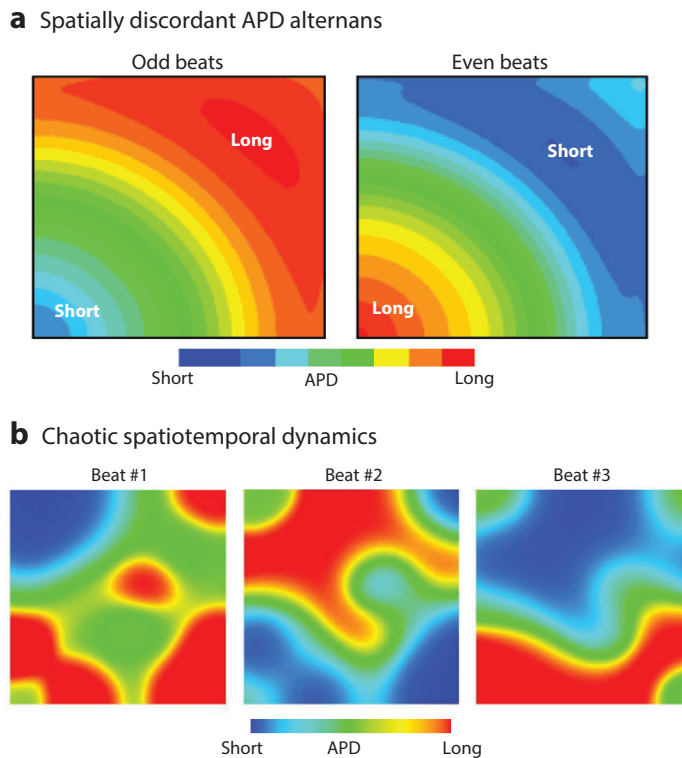


Figure 4

Dynamically induced dispersion of refractoriness. (*a*) Spatially discordant action potential duration (APD) alternans in which APD is short in one region but long in another region. In the following beat, the spatial APD pattern is reversed. (*b*) Spatiotemporal chaotic dynamics in the presence of early afterdepolarizations (EADs). The APD distribution in tissue exhibits an irregular spatial pattern and varies from beat to beat. EADs occur in long-APD regions (*red*), but not in short-APD regions (*blue*).

properties. Moreover, dynamic instabilities can simultaneously generate triggers and create a heterogeneous substrate that is vulnerable to initiation of reentry by those same triggers. As Sato et al. (14) showed in tissue exhibiting EADs, chaos synchronization results in the formation of tissue islands exhibiting action potentials with EADs next to tissue regions exhibiting action potentials without EADs (**Figure 4b**). If the EADs in these islands have sufficient amplitude to generate triggered activity, the impulses propagate readily into the regions without EADs and may then be blocked when they encounter another island with a long APD, thereby inducing reentry or a mixture of multiple foci and reentry. In the presence of preexisting tissue heterogeneities, dynamic instabilities are generally potentiated, increasing the probability that triggers will induce reentry.

4. ARRHYTHMIA DYNAMICS AT THE CELLULAR SCALE

The tissue-scale wave dynamics are collective behaviors of the myocytes that form the tissue. A single myocyte can exhibit a variety of action potential dynamics, including APD and Ca^{2+} alternans, EADs, DADs, automaticity, and random and chaotic dynamics. Understanding the

cellular dynamics is key for understanding the mechanisms of arrhythmias because they are not only important for understanding the tissue-scale mechanisms but also important for mechanistically linking the molecular and subcellular dynamics to the tissue- and organ-scale dynamics.

4.1. Alternans

Pulsus alternans and T-wave alternans are commonly observed clinically and are recognized as precursors of cardiac arrhythmias (42, 43). Because the T-wave is a measure of repolarization in the ventricles, T-wave alternans corresponds to APD alternans at the cellular scale, at which the action potential exhibits a long-short-long-short pattern (**Figure 1f**).

APD alternans can be caused either by instabilities originating from voltage (voltage-driven alternans) or by instabilities originating from Ca^{2+} cycling (Ca^{2+} -driven alternans) (44). However, because voltage and Ca^{2+} are bidirectionally coupled, alternans is always influenced by both factors, although one may predominate over the other, depending on the specific setting.

Voltage-driven alternans can be classified into three categories, all of which are related to APD restitution properties. The first and the most widely studied case is rapid, pacing-induced APD alternans (**Figure 1f**), which is caused by a steep slope of the APD restitution curve at short diastolic intervals. Theoretically, when the slope of the APD restitution curve at the equilibrium state for a given pacing rate exceeds one, the equilibrium state becomes unstable, and the system transitions to a new state. The instability, combined with nonlinear properties of APD restitution, can eventually lead to a stable long-short-long-short alternating pattern (i.e., APD alternans) or to much more complex periodic and frankly chaotic patterns (45, 46). Even though APD restitution is a collective property that arises from the recovery of all ionic currents and their interactions with voltage, the kinetics of recovery of $I_{\text{Ca,L}}$ is a particularly key factor regulating the steepness of APD restitution curve at fast heart rates (diastolic interval < 100 ms), because its recovery time constant is typically in this range of the diastolic interval (47). However, all other currents also contribute to the steepness of APD restitution either directly as a result of their own recovery from inactivation kinetics or indirectly by affecting other currents influencing the APD.

A second mechanism of voltage-driven alternans is transient outward K^+ current (I_{to})-driven APD alternans, which occurs at slow or normal heart rates. This type of alternans was first observed in ischemic tissue by Lukas & Antzelevitch (48) and later in a computer model by Hopfenfeld (49), who showed that alternans is induced by the sensitive dependence of the spike-and-dome action potential morphology on I_{to} . This mechanism of alternans can be responsible for the T-wave alternans seen in patients with Brugada syndrome (50). The mechanism of this type of alternans is also related to the steepness of APD restitution. However, due to short-term memory effects, the slope of APD restitution curve alone is not an accurate predictor (44). In addition to I_{to} , the slow component of the delayed rectifier K^+ current (I_{Ks}) also plays an important role due to its slow recovery kinetics.

The third mechanism of voltage-driven alternans is APD alternans at normal or slow heart rates caused by the interaction of window and pedestal $I_{\text{Ca,L}}$ with I_{Ks} , which can cause the T-wave alternans seen in patients with LQT syndrome (50). Under normal conditions, APD does not change dramatically at slow heart rates, because most of the ion channels are fully recovered. However, under the conditions of reduced repolarization reserve causing EADs, such as in LQT syndrome, APD varies sensitively with heart rate (51), causing alternans and more complex patterns at slow heart rates (52). The two major ionic currents critical to this slow-rate instability are the window and pedestal components of $I_{\text{Ca,L}}$ and I_{Ks} . Late I_{Na} [a persistent small conductance due to incomplete inactivation of the Na^+ channel (53–55)] can substitute for or enhance the role of window and pedestal $I_{\text{Ca,L}}$.

For Ca^{2+} -driven alternans, two mechanisms have been characterized (56, 57). In the first mechanism, alternans is caused by a steep fractional SR Ca^{2+} release relationship, first proposed by Eisner et al. (58). Later theoretical analyses (45, 59) showed that, besides a steep fractional SR release relationship, reduced SERCA pump activity is also required. A condition required by this mechanism is that SR Ca^{2+} load alternates concomitantly with cytosolic Ca^{2+} , which was observed in experiments from Eisner's group (60, 61) and others (62). However, later experimental studies also showed that this condition is not met under all circumstances and that cytosolic Ca^{2+} alternans can occur without SR Ca^{2+} load alternans (63, 64). That is, before each beat, the SR loads to the same level, but the amount of Ca^{2+} released exhibits an alternating pattern. These observations supported a different mechanism, in which refractoriness of the Ca^{2+} release channels (RyRs) is the major factor promoting alternans. Under such conditions, SR Ca^{2+} load alternans is not required. Refractoriness alone, however, is not sufficient to induce alternans, unless coupling of the Ca^{2+} release units is also present to allow a Ca^{2+} spark from one Ca^{2+} release unit to recruit a neighboring Ca^{2+} release unit to fire (65–67).

Alternans not only is a precursor but also can be a direct cause of arrhythmias. First, when APD alternans occurs, conduction block can occur at much slower pacing rates due to the long APD on alternate beats (45). Second, in cardiac tissue, APD alternans can be out of phase in different regions, forming spatially discordant APD alternans (**Figure 4a**), resulting in a large dispersion of refractoriness that creates a substrate vulnerable to initiation of reentry (68). Theoretical studies (40, 41) supported by experimental observations (69, 70) show that the formation of spatially discordant alternans requires conduction velocity restitution (**Supplemental Figure 2c**), i.e., a dependence of conduction velocity on its preceding diastolic interval. Because conduction velocity restitution is determined mainly by the recovery of Na^+ channels at very short diastolic intervals, spatially discordant alternans is a cause of arrhythmias only at very fast heart rates in the normal heart (>300 beats per min, as in pacing-induced VF). However, in the presence of Na^+ channel-blocking drugs that slow recovery from inactivation (71), during acute ischemia, or in electrically remodeled diseased hearts, spatially discordant alternans may develop at much slower heart rates (72).

4.2. Early Afterdepolarizations

EADs are voltage oscillations during the plateau and repolarization phases of the action potential (**Figure 1e**) and occur in cardiac diseases such as acquired and congenital LQT syndrome (73, 74) and heart failure (75, 76). In general, EADs occur when outward currents are reduced and/or inward currents are increased (77–80), a condition termed reduced repolarization reserve (81). However, whereas reduced repolarization reserve is sufficient to prolong APD, it is not sufficient to produce EADs. Other conditions are required to generate the voltage oscillations pathognomonic of EADs, which arise from different causes. These conditions are summarized in a recent review article (82) providing a holistic analysis of underlying mechanisms based on nonlinear dynamics. Even though each of the ionic currents in a cardiac myocyte can affect EADs, the most critical to the dynamics of oscillations include window $I_{\text{Ca,L}}$, late I_{Na} , and I_{Ks} . In addition, EADs can also be promoted by intracellular Ca^{2+} oscillations (83, 84) or by prolonged Ca^{2+} transients inducing EADs during the rapid repolarization phase of the action potential (phase 3 EADs) via I_{NCX} (85, 86).

A very interesting property of EADs is their sensitive all-or-nothing behavior in response to heart rate changes (**Supplemental Figure 5a**), which result in a steep, nonlinear APD restitution property (**Supplemental Figure 5b**). This nonlinear property can give rise to dynamic chaos (**Supplemental Figure 5c**) (14, 18), which is responsible for the irregularly appearing EAD behavior widely observed in experiments (**Supplemental Figure 5d**). The consequence of the chaotic dynamics at the tissue scale is the induction of dispersion of refractoriness. The dispersion of

refractoriness arises from the competition between the chaotic dynamics at the cellular level, which tends to create APD dispersion between cells, and the gap junction coupling at the tissue level, which forces APD to be regionally quasi-uniform. As a result, the chaotic EAD behavior becomes synchronized regionally but desynchronized globally, forming islands of long action potentials with EADs separated by regions without EADs (**Figure 4b**). The presence of preexisting tissue heterogeneity further amplifies this effect. In regions where EADs are too small to propagate, they create dispersion of refractoriness resulting in a tissue substrate vulnerable to reentry; in regions where EADs reach the threshold to propagate (e.g., **Figure 3c**), they generate triggers to initiate reentry. Depending on the cellular and tissue properties, this behavior can result in purely reentrant arrhythmias, multiple shifting foci, and a mixture of multiple shifting foci and reentry (14, 17).

4.3. Delayed Afterdepolarizations

DADs are spontaneous depolarizations during diastole that often occur following a train of rapid pacing (**Figure 1e**) (87). DADs are caused by spontaneous Ca^{2+} release from the SR that propagates as a Ca^{2+} wave through the myocyte (**Supplemental Figure 6a**) (88, 89). During a Ca^{2+} wave, cytoplasmic free Ca^{2+} concentration is elevated, which increases inward I_{NCX} and other Ca^{2+} -sensitive inward currents, causing a depolarization. If the voltage elevation does not reach the threshold for I_{Na} activation, there is only a small voltage deflection. Once the threshold for I_{Na} activation is exceeded, an action potential is elicited (**Figure 1e**). The magnitude of a DAD depends on the magnitude of the Ca^{2+} transient and the conductance of I_{NCX} and I_{K1} (90, 91). DADs are easier to induce in heart failure (91, 92) and CPVT (20, 93–96) than in normal hearts. In both heart failure and CPVT, RyRs become leaky, promoting spontaneous Ca^{2+} waves when the SR becomes Ca^{2+} loaded, e.g., by fast heart rates and adrenergic stimulation. In heart failure, I_{NCX} is upregulated and I_{K1} is downregulated, giving rise to favorable conditions for the formation of superthreshold DADs. The formation of Ca^{2+} waves is a self-organizing critical phenomenon (97, 98), exhibiting large fluctuations and thus resulting in the irregular occurrence of DADs (**Supplemental Figure 6b**). When a DAD triggers an action potential, it can result in a PVC, but when a DAD does not trigger an action potential, it may still create dispersion of excitability, promoting regional conduction block (99). Subthreshold DADs manifest as a U-wave on the electrocardiogram (100, 101). A key issue that still remains to be elucidated is how irregular DADs become synchronized regionally in tissue to induce arrhythmias (102, 103).

 Supplemental Material

4.4. Spike-and-Dome Action Potentials and Early Repolarization

In the ventricles, the higher I_{to} density in epicardial myocytes produces a characteristic spike-and-dome action potential morphology (**Figure 1b**) (104). Even though I_{to} is an outward current, it can prolong APD via secondary effects on other ion channels (105). If I_{to} is too large, however, the action potential abruptly shortens and loses the spike-and-dome morphology (**Supplemental Figure 4a,b**). Due to this steep, nonmonotonic response, alternans and irregular (chaotic) action potential dynamics can occur, as shown in experiments (48) and simulation studies (44, 49, 106, 107). When I_{to} is heterogeneously distributed, the region with the spike-and-dome action potential can propagate during phase 2 into the region with early repolarization and very short APD, inducing phase 2 reentry (**Supplemental Figure 4c**). In computer simulation studies of tissue exhibiting action potential heterogeneity due to I_{to} gradients, phase 2 reentry can be induced over a wide range of parameter space when irregular (chaotic) action potential dynamics are present (106, 107), whereas the parameter space is very narrow otherwise (108). Phase 2 reentry has been

demonstrated experimentally (37, 109) and is thought to be a major mechanism of arrhythmias during acute ischemia and in Brugada syndrome (110), although other factors, such as regional fibrosis promoting slow conduction, have also been proposed (111).

4.5. Automaticity

Under normal conditions, ventricular myocytes are excitable cells that remain at rest in the absence of a physiological pacemaker or electrical stimulus. However, ventricular myocytes can become oscillatory under abnormal conditions, termed automaticity (**Figure 1g**), which can generate PVCs or repetitive focal excitations in tissue. Multiple factors can cause automaticity. For example, Na^+ channel inactivation defects, such as aconitine-induced automaticity (112), or I_{K1} reduction (113), cause spontaneous beating. Coupling of myocytes to myofibroblasts via heterocellular gap junctions can also depolarize the myocyte's resting membrane potential sufficiently to induce automaticity (114), which may be relevant to the increased ventricular ectopy seen in diseased hearts with fibrosis. Periodic Ca^{2+} oscillations, similar to the mechanisms causing DAD-mediated triggered activity, can also result in automaticity. The bidirectional coupling of voltage and Ca^{2+} (i.e., voltage affects Ca^{2+} at the same time that Ca^{2+} affects voltage) potentiates this mechanism such that spontaneous Ca^{2+} release elicits an action potential, and consequently, the action potential brings in more Ca^{2+} through Ca^{2+} channels to enhance spontaneous Ca^{2+} release. This coupling process forms a positive feedback loop in a manner similar to that of the Ca^{2+} oscillation that drives the sinoatrial node (115). A third mechanism is similar to that of EADs, in which oscillations mediated by $I_{\text{Ca,L}}$ during the plateau become sustained due to failure of full repolarization (30).

4.6. Dynamics Arising from Heterocellular Coupling

The cellular dynamics summarized above do not always arise from myocytes but can emerge from heterocellular coupling of myocytes to nonmyocytes. For example, coupling of a myocyte to a fibroblast/myofibroblast through heterocellular gap junctions can result in automaticity (114), EADs (116), spike-and-dome action potential morphology, and alternans (117). Normal excitable ventricular cells coupled to nonexcitable ischemic ventricular cells may result in sustained oscillations (118). Two cells with different APDs under conditions of reduced repolarization reserve can also result in EADs (36).

5. SUBCELLULAR DYNAMICS AND THE MOLECULAR AND IONIC BASIS OF ARRHYTHMIAS

The cellular dynamics and the corresponding dynamic parameters (e.g., APD, APD restitution, conduction velocity, and conduction velocity restitution) are properties that emerge from the nonlinear interactions between multiple molecular and ionic factors (**Figure 5**). For example, APD restitution is not controlled by a single current but is a collective behavior of the recovery of all ionic currents and their interactions with voltage. However, some currents have greater influence than others. Moreover, molecular interactions at the subcellular scale, such as Ca^{2+} alternans and Ca^{2+} waves that influence the cellular dynamics through their aggregate effects on ionic currents, create subcellular dynamics. Although complex, the situation is not hopelessly so. Each molecular factor plays a specific role in promoting dynamics that can ultimately be dissected by a combined approach integrating nonlinear dynamics, modeling, and experiment. Here we briefly summarize the roles of some of the key molecular factors promoting the subcellular and cellular dynamics.

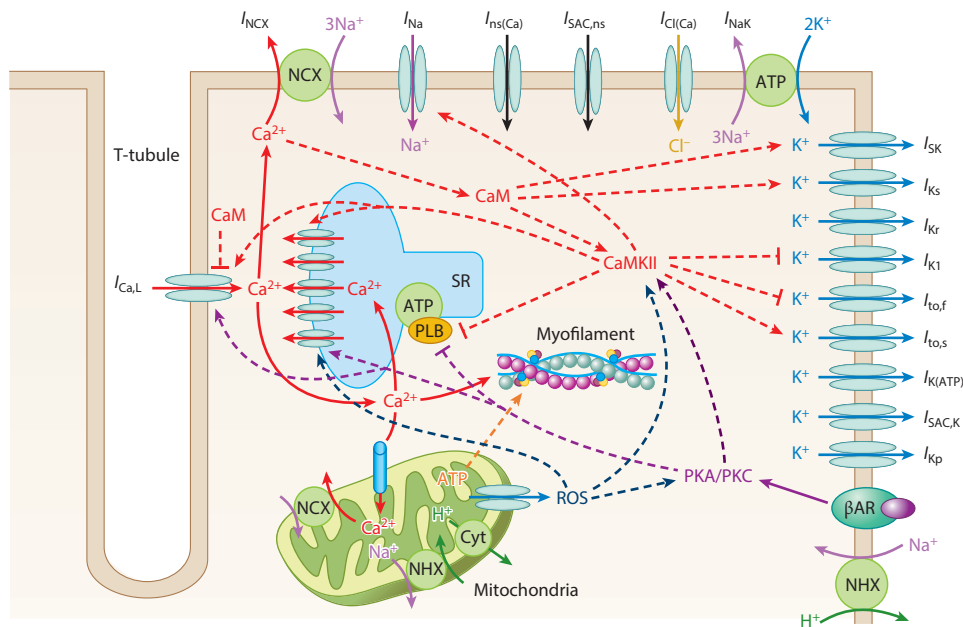


Figure 5

Schematic diagram of ionic currents, transporters, signaling pathways, and their interactions in a ventricular myocyte. A dashed line with arrow indicates that signaling enhances activity, and a dashed line with bar indicates suppression of activity. See text for details.

5.1. Ion Channels and Transporters

There are many types of ion channels and transporters in the membranes of a ventricular myocyte (**Figure 5**). Alterations of the ion channel and transporter properties may result in cellular action potential dynamics that lead to arrhythmias at the tissue and organ scales. Here we review their specific roles in generating the cellular action potential dynamics.

5.1.1. Na^+ channels. I_{Na} is the main current responsible for the rapid upstroke of the action potential in ventricular myocytes. By determining the speed of the upstroke (dV/dt_{max}), I_{Na} is a major determinant of excitability and conduction velocity. For this reason, I_{Na} (specifically its recovery from inactivation) largely determines conduction velocity restitution, which is exacerbated in chronic ischemia by slowed recovery from inactivation (119). I_{Na} affects APD indirectly and directly. The amplitude of I_{Na} determines the maximum voltage of the action potential, which affects voltage-dependent activation of other currents influencing action potential repolarization. I_{Na} therefore contributes to APD restitution at very short diastolic intervals when its recovery from inactivation is still incomplete, which in turn affects the stability of reentry. I_{Na} properties also become altered under diseased conditions, failing to inactivate fully during the action potential and thus resulting in late I_{Na} . Late I_{Na} can result from genetic mutations in Na^+ channels, causing LQT3 syndrome, or can be induced by signaling pathways such as Ca^{2+} /calmodulin-dependent protein kinase II (CaMKII) (**Figure 5**) (53), which is activated in heart failure. Late I_{Na} directly prolongs APD and can cause EADs by reducing repolarization reserve. Moreover, late I_{Na} brings extra Na^+ into the cell, which increases intracellular Na^+ and thus intracellular Ca^{2+} via Na^+ - Ca^{2+} exchangers. Elevation of Ca^{2+} can promote Ca^{2+} alternans and waves and further

activate the CaMKII signaling pathway, generating more late I_{Na} in a positive feedback loop, with arrhythmogenic consequences (53–55).

5.1.2. L-type Ca^{2+} channels. L-type Ca^{2+} channels play two major roles under normal conditions: triggering Ca^{2+} release from the SR essential for contraction and maintaining the plateau phase of the action potential. Due to the latter, $I_{Ca,L}$ is a major determinant of APD and thus APD restitution. More importantly, because the time constant of recovery of $I_{Ca,L}$ is less than 100 ms, $I_{Ca,L}$ has a major effect on the steepness of APD restitution at short to intermediate diastolic intervals. Thus, $I_{Ca,L}$ plays an important role in the development of APD alternans at fast heart rates, as well as in spiral wave stability. Blocking $I_{Ca,L}$ suppresses APD alternans and prevents spiral wave breakup (26). The late component of $I_{Ca,L}$ (termed the window and pedestal $I_{Ca,L}$), although relatively small compared with peak $I_{Ca,L}$, plays a key role in promoting EADs (78, 120), as well as APD alternans at slow heart rates (52). In addition, increasing $I_{Ca,L}$ increases Ca^{2+} entry and thus promotes intracellular Ca^{2+} loading, which can promote Ca^{2+} alternans and waves, as well as activating the CaMKII signaling pathway. $I_{Ca,L}$ is regulated by Ca^{2+} in two ways (Figure 5): Ca^{2+} binds with calmodulin to form a Ca^{2+} /calmodulin complex, which causes Ca^{2+} -dependent inactivation to decrease $I_{Ca,L}$, forming a negative feedback loop, and activation of the CaMKII pathway increases $I_{Ca,L}$, forming a positive feedback loop.

5.1.3. K^+ channels. There are a wide variety of K^+ currents in ventricular myocytes (121) (Figure 5), including the fast and slow I_{to} ($I_{to,f}$ and $I_{to,s}$), the fast and slow components of the delayed rectifier K^+ current (I_{Kr} and I_{Ks}), I_{K1} , the plateau K^+ current (I_{Kp}), ATP-sensitive K^+ current [$I_{K(ATP)}$], stretch-activated K^+ current ($I_{SAC,K}$), and small-conductance Ca^{2+} -activated K^+ current (I_{SK}) (122–124). The common role of K^+ currents is to facilitate repolarization of the action potential such that reducing these currents generally lengthens APD. In general, reducing K^+ currents has a larger effect on lengthening APD at slow heart rates than at fast heart rates, resulting in a steeper APD restitution curve, which promotes alternans and spiral wave instability. The reduction in repolarization reserve also promotes EAD-mediated arrhythmias. Due to their different kinetics and Ca^{2+} dependencies, however, different K^+ currents play different roles in promoting these arrhythmogenic dynamics. For example, by enhancing early repolarization reserve, I_{to} lowers the early plateau voltage into the window range of $I_{Ca,L}$ and slows the activation of I_{Ks} , paradoxically reducing late repolarization reserve and promoting EADs (125). In contrast, I_{Ks} activates and deactivates very slowly, thereby preferentially lengthening APD at slow heart rates, which plays a major role in EAD formation. Under conditions of reduced repolarization reserve, slow deactivation of I_{Ks} plays a major role in steepening APD restitution at slow heart rates, which promotes APD alternans at slow heart rates (52). I_{K1} is a time-independent current responsible for phase 3 (rapid repolarization) of the action potential as well as for maintaining a stable diastolic resting potential. Therefore, I_{K1} , like I_{Na} , is a major determinant of both excitability and conduction velocity. For this reason, reduction of I_{K1} is an important contributor to DADs (91), as well as to automaticity (113).

When K^+ currents are enhanced, in contrast, increased repolarization reserve can also promote arrhythmogenic dynamics by different mechanisms. I_{to} produces the spike-and-dome morphology required for phase 2 reentry when repolarization reserve is increased due to either enhanced K^+ conductance or decreased inward conductance, as in Brugada syndrome and short-QT syndrome characterized by gain-of-function mutations in K^+ channels or loss-of-function mutations in Na^+ or Ca^{2+} channels (126). Activation of $I_{K(ATP)}$ serves a similar role in acute ischemia by summing with I_{to} to induce early repolarization promoting phase 2 reentry (37). In addition, mitochondrial depolarization causing $I_{K(ATP)}$ activation during acute ischemia/reperfusion has been proposed to

generate regional metabolic sinks that enhance electrical dispersion and create a tissue substrate vulnerable to reentry (127). Recent studies (123, 124) show that I_{SK} , normally expressed in atrial tissue, becomes upregulated in ventricular tissue during heart failure and may promote ventricular arrhythmias by shortening APD relative to the Ca^{2+} transient, promoting EADs in the late part of phase 3 (85, 86, 123, 128).

5.1.4. Ion transporters. Maintaining proper ion gradients across the cell membrane is required for cardiac myocytes to remain excitable and oscillatory. To maintain intracellular ion concentrations, Na^+-Ca^{2+} exchange transports one Ca^{2+} ion for three Na^+ ions, and Na^+-K^+ ATPase transports three Na^+ ions for two K^+ ions. Because both transporters are electrogenic, they affect both action potential and Ca^{2+} cycling dynamics. I_{NCX} prolongs APD and can promote EADs and is also a key player in DADs (91, 129) and automaticity (113). Blocking the Na^+-K^+ pump current (I_{NaK}) causes intracellular Na^+ elevation, which promotes intracellular Ca^{2+} loading via the Na^+-Ca^{2+} exchanger, Ca^{2+} waves, and thus DADs (130).

5.1.5. Miscellaneous ion channels and transporters. Other ion channels and transporters in ventricular myocytes may also play important roles in cellular dynamics. For example, Ca^{2+} -activated nonselective cation channels [$I_{ns(Ca)}$] (14), Ca^{2+} -activated Cl^- channels [$I_{Cl(Ca)}$] (131), and stretch-activated nonselective cation channels [$I_{SAC,ns}$] (132) are inward currents, which may contribute to EAD and DAD formation, as well as influencing repolarization and affecting APD restitution properties. Ion channels and transporters located in intracellular organelles, such as RyRs and SERCA in the SR and a variety of ion channels in mitochondria, also play critical roles in regulating subcellular Ca^{2+} cycling and cardiac energetics. These channels and transporters indirectly affect subcellular and cellular arrhythmia dynamics by modulating the properties of sarcolemmal ion channels and transporters, as discussed in more detail in the next section.

5.2. Ionic Homeostasis and Subcellular Ca^{2+} Cycling Dynamics

Intracellular Ca^{2+} cycling plays multiple critical roles in cardiac arrhythmias (88, 133). First, Ca^{2+} levels during systole and diastole directly affect Ca^{2+} -dependent ionic currents, such as $I_{Ca,L}$, I_{NCX} , I_{Ks} , and I_{SK} , which then modulate cellular action potential dynamics. Second, Ca^{2+} regulates Ca^{2+} -dependent signaling pathways, such as CaMKII, that in turn modulate ionic currents and Ca^{2+} cycling (Figure 5). Third, Ca^{2+} cycling can generate its own arrhythmogenic dynamics, including Ca^{2+} alternans and Ca^{2+} waves. As shown by recent studies, these dynamics are self-organizing phenomena of spatiotemporal systems. A ventricular myocyte contains more than 20,000 Ca^{2+} release units, which are coupled by Ca^{2+} diffusion via Ca^{2+} -induced Ca^{2+} release. Each Ca^{2+} release unit contains a RyR cluster in which the RyRs fire collectively, producing an all-or-nothing, localized Ca^{2+} release event termed a Ca^{2+} spark (134, 135). Ca^{2+} sparks are random events but also have their own complex dynamics (135–137). Ca^{2+} alternans is a self-organized phenomenon arising from the interaction of Ca^{2+} sparks (i.e., the coupling of Ca^{2+} release units), as analyzed in our recent theoretical studies (56, 65, 66). In addition, different patterns of spatiotemporal subcellular Ca^{2+} alternans dynamics, including spatially discordant alternans (138) and transition from microscopic alternans to macroscopic alternans (139), have been demonstrated. The transition from Ca^{2+} sparks to Ca^{2+} waves reflects a signaling hierarchy: individual sparks, spark clusters, abortive waves, and persistent waves (140, 141), which can be described by the theory of criticality (97, 98). Three general properties of a diffusively coupled Ca^{2+} release unit network can account for the essential dynamics: random activation, refractoriness, and recruitment [the 3R theory (56)]. Self-organized criticality can be used to explain why Ca^{2+} waves occur much later than RyR recovery and SR refilling time, a time delay termed the idle period

(142). In the formation of both Ca^{2+} alternans and Ca^{2+} waves, the coupling of Ca^{2+} release units plays a key role.

Dysregulation of intracellular Na^+ can also promote arrhythmogenic dynamics (143). Elevation of intracellular Na^+ enhances the Na^+ - K^+ pump (increasing outward I_{NaK}) but slows intracellular Ca^{2+} removal by Na^+ - Ca^{2+} exchange (decreasing inward I_{NCX}). These effects tend to shorten the action potential and elevate intracellular Ca^{2+} , which can promote arrhythmogenic Ca^{2+} cycling dynamics. The presence of late I_{Na} can cause Na^+ overload, which then causes Ca^{2+} overload, facilitating CaMKII activation. CaMKII activation in turn amplifies late I_{Na} in a positive feedback loop, potentiating arrhythmia dynamics (53–55).

K^+ (particularly extracellular K^+) also affects arrhythmia dynamics. Normal extracellular $[\text{K}^+]$ concentration is 3.5 to 5 mM, and both lower and higher extracellular $[\text{K}^+]$ can cause arrhythmias. Specifically, elevation of extracellular $[\text{K}^+]$ depolarizes resting membrane potential and increases I_{K1} and I_{Kr} , which shortens the action potential. Elevation of the resting potential first increases and then slows conduction velocity, eventually resulting in conduction failure. In contrast, lowering extracellular $[\text{K}^+]$ decreases I_{K1} and I_{Kr} , which lengthens APD and destabilizes the resting potential. Lengthening APD can promote EADs, as well as increased Ca^{2+} loading. Lowering extracellular $[\text{K}^+]$ also inhibits the Na^+ - K^+ pump, further promoting Na^+ and Ca^{2+} overload. Ca^{2+} overload can then activate the CaMKII signaling pathway, which further potentiates Na^+ and Ca^{2+} loading by increasing late I_{Na} and $I_{\text{Ca,L}}$. These effects act synergistically to promote arrhythmogenic cellular action potential dynamics, such as alternans, EADs, and DADs.

5.3. Genetic Factors

Genetic mutations in ion channels, transporters, and their regulatory and trafficking partners that predispose to cardiac arrhythmias have provided powerful insights illuminating the molecular basis of cardiac arrhythmias (4, 5). Although too broad a field to review in detail here, channelopathies that are caused by gene mutations, such as LQT syndrome, CPVT, short-QT syndrome, and Brugada syndrome, have been highly informative. So far, 13 genes for LQT, 4 genes for CVPT, and 7 genes for Brugada syndrome, with hundreds of mutations, have been identified (126, 144). A mutation may cause gain or loss of function that affects action potential or Ca^{2+} cycling dynamics through the dynamic mechanisms outlined above. For example, LQT mutations lengthen APD and predispose the myocytes to EADs, whereas CPVT mutations increase the RyR open probability and predispose the myocytes to DADs. A single gene mutation may have multiple consequences for cellular dynamics and disease phenotypes. For example, Na^+ channel mutation 1795insD can cause both LQT syndrome and Brugada syndrome (145). Although genetic channelopathies are relatively rare, they share important commonalities with ventricular arrhythmias associated with common diseases. For example, arrhythmias in the setting of heart failure recapitulate features of LQT syndromes (e.g., reduced repolarization reserve promoting EAD-mediated arrhythmias such as polymorphic VT), and arrhythmias during acute ischemia recapitulate features of Brugada syndrome (phase 2 reentry). Both types of arrhythmias recapitulate features of CPVT (abnormal Ca^{2+} cycling promoting alternans, Ca^{2+} waves, and DAD-mediated arrhythmias).

5.4. Signaling Pathways

By modifying ion channel and transporter properties at the molecular level, a variety of signaling pathways critically influence arrhythmia dynamics (133, 146, 147–149), both acutely through post-translational modification of their protein targets (e.g., phosphorylation) and chronically by altering transcription, trafficking, and protein turnover (electrical remodeling, including gap junction

remodeling). In addition to their effects on sarcolemmal ion channels/transporters, these signaling pathways also regulate Ca^{2+} cycling elements both acutely and chronically (excitation-contraction coupling remodeling), as well as gap junction coupling (gap junction remodeling). These pathways alter cellular metabolism (metabolic remodeling) and influence (*a*) nonmyocytes such as fibroblasts (structural remodeling), (*b*) vascular components (vascular remodeling), and (*c*) neural components (neural remodeling). Although too broad a field to review here, the most widely studied signaling pathways include the adrenergic/cholinergic, angiotensin/aldosterone, and CaMKII/calcineurin axes. They promote arrhythmias through their effects on Ca^{2+} cycling and ionic currents, as well as through modifying tissue coupling properties. **Figure 5** plots part of the signaling pathways of protein kinases A and C and CaMKII and their effects on the SERCA pump, RyRs, and many ionic currents. By destabilizing subcellular-, cellular-, and tissue-scale dynamics and exacerbating tissue heterogeneity, these signaling pathways play a key role in increasing the susceptibility of the heart to arrhythmias.

6. CONCLUDING REMARKS

As this article reviews, cardiac dynamics are regulated by multiple factors operating over different temporal and spatial scales in a complex interactive network. We can briefly summarize the important general concepts as follows. First, molecular-scale events, such as genetic mutations, signaling, and metabolism, regulate ion channel and Ca^{2+} cycling properties. Second, the ionic currents determine the action potential and intracellular ion concentrations, but they are also regulated by voltage and ion concentrations as well as by signaling pathways. Third, Ca^{2+} cycling can independently give rise to arrhythmogenic subcellular and cellular dynamics. Fourth, because Ca^{2+} and voltage are bidirectionally coupled, the feedback loops between them give rise to a rich variety of cellular action potential dynamics. Fifth, the cellular action potential dynamics combined with tissue-scale factors promote tissue-scale dynamics, creating tissue substrates that generate focal excitations and are susceptible to initiation of reentry due to electrical dispersion. Sixth, the systems dynamics at the organism scale activate reflexes that feed back to the molecular level through activation of a variety of signaling pathways. Finally, even though these multiscale interactions are very complex, the two key hubs are voltage and Ca^{2+} . Understanding the action potential and Ca^{2+} cycling dynamics is critical for relating molecular-scale events to the development of ventricular arrhythmias.

Table 1 summarizes our current understanding of the subcellular, cellular, and tissue-scale action potential and Ca^{2+} cycling dynamics, their corresponding mechanisms, their electrocardiographic characteristics, and their link to clinical diseases. We hope that this can be a useful platform that will facilitate the quest to move beyond engineering approaches (devices and ablation) to treat ventricular arrhythmias and to move toward the development of novel biological approaches. In this quest, we note that, even in the normal heart, lethal arrhythmias can be induced by rapid pacing or electrical shocks. In other words, from a dynamics perspective, both sinus rhythm and arrhythmias are solutions of the normal heart as well as the diseased heart. The occurrence of arrhythmias is a probabilistic transition from sinus rhythm to turbulent ventricular behavior. In the view of nonlinear dynamics, the objective of an effective therapy is to elevate the threshold governing the transition from sinus rhythm to arrhythmias without markedly altering normal sinus rhythm, i.e., to enlarge the basin of attraction of normal sinus rhythm while suppressing the basin of attraction of arrhythmias.

To achieve this goal, however, there are considerable challenges to overcome. First, a given molecular target, such as an ion channel, often has effects on multiple aspects of arrhythmia dynamics such that a drug effective at treating one mechanism may worsen another, potentially

Table 1 From subcellular/cellular/tissue dynamics to arrhythmias

Cellular (subcellular) dynamics	Tissue dynamics	Dynamic mechanisms/parameters	ECG characteristics	Related disease conditions
APD and Ca ²⁺ alternans, chaos	APD and Ca ²⁺ alternans, DOR, reentry	Steep APDR and CVR, steep FSRCR, 3R theory	TWA	LQTS, BS, HF, ischemia
EAD (Ca ²⁺ oscillations)	Foci, DOR, biexcitability	RRR, Hopf bifurcation, steep APDR, chaos synchronization	PVC, TWA, NSVT, TdP	LQTS, HF
DAD (Ca ²⁺ wave)	Foci	Criticality, synchronization	PVC, U-wave	CPVT, HF
Spike-and-dome	Phase 2 reentry	ERR, APDR, chaos	TWA, J-wave	BS, ERS, SQTS, acute ischemia
Automaticity (Ca ²⁺ oscillations)	Foci	Hopf bifurcation, synchronization	PVC, NSVT	Idioventricular rhythms

Abbreviations: 3R theory, theory of Ca²⁺ alternans involving random activation, refractoriness, and recruitment of Ca²⁺ release units; APD, action potential duration; APDR, APD restitution; BS, Brugada syndrome; CPVT, catecholaminergic polymorphic ventricular tachycardia; CVR, conduction velocity restitution; DAD, delayed afterdepolarization; DOR, dispersion of refractoriness; EAD, early afterdepolarization; ECG, electrocardiogram; ERR, enhanced repolarization reserve; ERS, early repolarization syndrome; FSRCR, fractional sarcoplasmic reticulum Ca²⁺ release; HF, heart failure; LQTS, long-QT syndrome; NSVT, nonsustained ventricular tachycardia; PVC, premature ventricular complex; RRR, reduced repolarization reserve; SQTS, short-QT syndrome; TdP, torsade de pointes; TWA, T-wave alternans.

substituting one lethal arrhythmia for another. For example, class I antiarrhythmic drugs, which block Na⁺ channels, can successfully suppress PVCs. The CAST trial (6) was designed to test the hypothesis that suppressing PVCs with class I antiarrhythmic drugs would reduce mortality by reducing arrhythmia triggers. However, such drugs also lower excitability, especially in ischemic hearts, enhancing the vulnerability of the tissue substrate to reentry, which led to a higher death rate in the treated group in the CAST trial (6). Class III antiarrhythmic drugs, which block K⁺ channels, lengthen APD to prevent reentry. The SWORD trial (7) was designed to test the hypothesis that lengthening APD with class III antiarrhythmic drugs would reduce mortality by preventing reentry. However, these drugs also reduce repolarization reserve and promote EADs, which may have caused increased mortality in the treated group in the SWORD trial (7). Therefore, the ideal therapeutic intervention should suppress all dynamic mechanisms of arrhythmias described above or, at the very least, suppress one without exacerbating the others. Second, the occurrence of arrhythmias, especially VF, is unpredictable. These events are rare events, even when potential triggering events such as PVCs are common. One of the greatest challenges is to predict which patients are at the highest risk and need to be treated, whether by biologics or device therapy. In our view, future efforts not only should focus on specific arrhythmia mechanisms but also should require a systems view of ventricular arrhythmias to accurately predict arrhythmia risk, to identify the right therapeutic targets, and to develop effective and robust therapeutics.

DISCLOSURE STATEMENT

The authors are not aware of any affiliations, memberships, funding, or financial holdings that might be perceived as affecting the objectivity of this review.

LITERATURE CITED

1. Janse MJ, Rosen MR. 2006. History of arrhythmias. *Handb. Exp. Pharmacol.* 2006:1–39
2. Jalife J. 2000. Ventricular fibrillation: mechanisms of initiation and maintenance. *Annu. Rev. Physiol.* 62:25–50

3. Zipes DP, Wellens HJ. 1998. Sudden cardiac death. *Circulation* 98:2334–51
4. Priori SG, Napolitano C. 2004. Genetics of cardiac arrhythmias and sudden cardiac death. *Ann. N. Y. Acad. Sci.* 1015:96–110
5. Marsman RF, Tan HL, Bezzina CR. 2014. Genetics of sudden cardiac death caused by ventricular arrhythmias. *Nat. Rev. Cardiol.* 11:96–111
6. CAST I. 1989. Effect of encainide and flecainide on mortality in a random trial of arrhythmia suppression after myocardial infarction. *N. Engl. J. Med.* 321:406–12
7. Waldo AL, Camm AJ, deRuyter H, Friedman PL, Macneil DJ, et al. 1996. Effect of d-sotalol on mortality in patients with left ventricular dysfunction after recent and remote myocardial infarction. *Lancet* 348:7–12
8. Myerburg RJ, Mitrani R, Interian A, Castellanos A. 1998. Interpretation of outcomes of antiarrhythmic clinical trials: design features and population impact. *Circulation* 97:1514–21
9. Tung R, Zimetbaum P, Josephson ME. 2008. A critical appraisal of implantable cardioverter-defibrillator therapy for the prevention of sudden cardiac death. *J. Am. Coll. Cardiol.* 52:1111–21
10. Qu Z, Hu G, Garfinkel A, Weiss JN. 2014. Nonlinear and stochastic dynamics in the heart. *Phys. Rep.* 543:61–162
11. O'Reilly CM, Fogarty KE, Drummond RM, Tuft RA, Walsh JV. 2003. Quantitative analysis of spontaneous mitochondrial depolarizations. *Biophys. J.* 85:3350–57
12. Aon MA, Cortassa S, Marban E, O'Rourke B. 2003. Synchronized whole cell oscillations in mitochondrial metabolism triggered by a local release of reactive oxygen species in cardiac myocytes. *J. Biol. Chem.* 278:44735–44
13. Xie Y, Sato D, Garfinkel A, Qu Z, Weiss JN. 2010. So little source, so much sink: requirements for afterdepolarizations to propagate in tissue. *Biophys. J.* 99:1408–15
14. Sato D, Xie LH, Sovari AA, Tran DX, Morita N, et al. 2009. Synchronization of chaotic early afterdepolarizations in the genesis of cardiac arrhythmias. *PNAS* 106:2983–88
15. Asano Y, Davidenko JM, Baxter WT, Gray RA, Jalife J. 1997. Optical mapping of drug-induced polymorphic arrhythmias and torsade de pointes in the isolated rabbit heart. *J. Am. Coll. Cardiol.* 29:831–42
16. Choi B-R, Burton F, Salama G. 2002. Cytosolic Ca²⁺ triggers early afterdepolarizations and torsade de pointes in rabbit hearts with type 2 long QT syndrome. *J. Physiol.* 543:615–31
17. de Lange E, Xie Y, Qu Z. 2012. Synchronization of early afterdepolarizations and arrhythmogenesis in heterogeneous cardiac tissue models. *Biophys. J.* 103:365–73
18. Sato D, Xie LH, Nguyen TP, Weiss JN, Qu Z. 2010. Irregularly appearing early afterdepolarizations in cardiac myocytes: random fluctuations or dynamical chaos? *Biophys. J.* 99:765–73
19. Qu Z. 2011. Chaos in the genesis and maintenance of cardiac arrhythmias. *Prog. Biophys. Mol. Biol.* 105:247–57
20. Cerrone M, Noujaim SF, Tolkacheva EG, Talkachou A, O'Connell R, et al. 2007. Arrhythmogenic mechanisms in a mouse model of catecholaminergic polymorphic ventricular tachycardia. *Circ. Res.* 101:1039–48
21. Baher AA, Uy M, Xie F, Garfinkel A, Qu Z, Weiss JN. 2011. Bidirectional ventricular tachycardia: ping pong in the His–Purkinje system. *Heart Rhythm* 8:599–605
22. Mines GR. 1914. On circulating excitation on heart muscles and their possible relation to tachycardia and fibrillation. *Trans. R. Soc. Can.* 4:43–52
23. Winfree AT. 1972. Spiral waves of chemical activity. *Science* 175:634–36
24. Davidenko JM, Pertsov AM, Salomonsz R, Baxter W, Jalife J. 1992. Stationary and drifting spiral waves of excitation in isolated cardiac muscle. *Nature* 355:349–51
25. Qu Z, Xie F, Garfinkel A, Weiss JN. 2000. Origins of spiral wave meander and breakup in a two-dimensional cardiac tissue model. *Ann. Biomed. Eng.* 28:755–71
26. Wu TJ, Lin SF, Weiss JN, Ting CT, Chen PS. 2002. Two types of ventricular fibrillation in isolated rabbit hearts—importance of excitability and action potential duration restitution. *Circulation* 106:1859–66
27. Moe GK, Rheinboldt WC, Abildskov JA. 1964. A computer model of atrial fibrillation. *Am. Heart J.* 67:200–20

28. Chang MG, Sato D, de Lange E, Lee J-H, Karagueuzian HS, et al. 2012. Bi-stable wave propagation and early afterdepolarization-mediated cardiac arrhythmias. *Heart Rhythm* 9:115–22
29. Chang MG, de Lange E, Calmettes G, Garfinkel A, Qu Z, Weiss JN. 2013. Pro- and antiarrhythmic effects of ATP-sensitive potassium current activation on reentry during early afterdepolarization-mediated arrhythmias. *Heart Rhythm* 10:575–82
30. Vandersickel N, Kazbanov IV, Nuijtemans A, Weise LD, Pandit R, Panfilov AV. 2014. A study of early afterdepolarizations in a model for human ventricular tissue. *PLOS ONE* 9:e84595
31. Gadsby DC, Cranefield PF. 1977. Two levels of resting potential in cardiac Purkinje fibers. *J. Gen. Physiol.* 70:725–46
32. Yan G-X, Wu Y, Liu T, Wang J, Marinchak RA, Kowey PR. 2001. Phase 2 early afterdepolarization as a trigger of polymorphic ventricular tachycardia in acquired long-QT syndrome: direct evidence from intracellular recordings in the intact left ventricular wall. *Circulation* 103:2851–56
33. Nguyen TP, Qu Z, Weiss JN. 2014. Cardiac fibrosis and arrhythmogenesis: The road to repair is paved with perils. *J. Mol. Cell. Cardiol.* 70C:83–91
34. Rohr S, Kucera JP, Fast VG, Kleber AG. 1997. Paradoxical improvement of impulse conduction in cardiac tissue by partial cellular uncoupling. *Science* 275:841–44
35. Janse MJ, Wit AL. 1989. Electrophysiological mechanisms of ventricular arrhythmias resulting from myocardial ischemia and infarction. *Physiol. Rev.* 69:1046–169
36. Maruyama M, Lin SF, Xie Y, Chua SK, Joung B, et al. 2011. Genesis of phase 3 early afterdepolarizations and triggered activity in acquired long-QT syndrome. *Circ. Arrhythm. Electrophysiol.* 4:103–11
37. Lukas A, Antzelevitch C. 1996. Phase 2 reentry as a mechanism of initiation of circus movement reentry in canine epicardium exposed to simulated ischemia. *Cardiovasc. Res.* 32:593–603
38. Yan GX, Antzelevitch C. 1999. Cellular basis for the Brugada syndrome and other mechanisms of arrhythmogenesis associated with ST-segment elevation. *Circulation* 100:1660–66
39. Yan GX, Joshi A, Guo D, Hlaing T, Martin J, et al. 2004. Phase 2 reentry as a trigger to initiate ventricular fibrillation during early acute myocardial ischemia. *Circulation* 110:1036–41
40. Echebarria B, Karma A. 2002. Instability and spatiotemporal dynamics of alternans in paced cardiac tissue. *Phys. Rev. Lett.* 88:208101
41. Qu Z, Garfinkel A, Chen PS, Weiss JN. 2000. Mechanisms of discordant alternans and induction of reentry in simulated cardiac tissue. *Circulation* 102:1664–70
42. Rosenbaum DS, Jackson LE, Smith JM, Garan H, Ruskin JN, Cohen RJ. 1994. Electrical alternans and vulnerability to ventricular arrhythmias. *N. Engl. J. Med.* 330:235–41
43. Verrier RL, Klingenhoben T, Malik M, El-Sherif N, Exner DV, et al. 2011. Microvolt T-wave alternans physiological basis, methods of measurement, and clinical utility—consensus guideline by International Society for Holter and Noninvasive Electrocardiology. *J. Am. Coll. Cardiol.* 58:1309–24
44. Qu Z, Xie Y, Garfinkel A, Weiss JN. 2010. T-wave alternans and arrhythmogenesis in cardiac diseases. *Front. Physiol.* 1:154
45. Qu Z, Shiferaw Y, Weiss JN. 2007. Nonlinear dynamics of cardiac excitation-contraction coupling: an iterated map study. *Phys. Rev. E* 75:011927
46. Chialvo DR, Gilmour RF, Jalife J. 1990. Low dimensional chaos in cardiac tissue. *Nature* 343:653–57
47. Mahajan A, Shiferaw Y, Sato D, Baher A, Olcese R, et al. 2008. A rabbit ventricular action potential model replicating cardiac dynamics at rapid heart rates. *Biophys. J.* 94:392–410
48. Lukas A, Antzelevitch C. 1993. Differences in the electrophysiological response of canine ventricular epicardium and endocardium to ischemia. Role of the transient outward current. *Circulation* 88:2903–15
49. Hopenfeld B. 2006. Mechanism for action potential alternans: the interplay between L-type calcium current and transient outward current. *Heart Rhythm* 3:345–52
50. Wegener FT, Ehrlich JR, Hohnloser SH. 2008. Amiodarone-associated macroscopic T-wave alternans and torsade de pointes unmasking the inherited long QT syndrome. *Europace* 10:112–13
51. Antzelevitch C. 2001. Heterogeneity of cellular repolarization in LQTS: the role of M cells. *Eur. Heart J. Suppl.* 3:K2–16
52. Qu Z, Chung D. 2012. Mechanisms and determinants of ultralong action potential duration and slow rate-dependence in cardiac myocytes. *PLOS ONE* 7:e43587

53. Wagner S, Ruff HM, Weber SL, Bellmann S, Sowa T, et al. 2011. Reactive oxygen species-activated Ca/calmodulin kinase II δ is required for late I_{Na} augmentation leading to cellular Na and Ca overload. *Circ. Res.* 108:555–65
54. Wasserstrom JA, Sharma R, O'Toole MJ, Zheng J, Kelly JE, et al. 2009. Ranolazine antagonizes the effects of increased late sodium current on intracellular calcium cycling in rat isolated intact heart. *J. Pharmacol. Exp. Ther.* 331:382–91
55. Song Y, Shryock JC, Belardinelli L. 2008. An increase of late sodium current induces delayed afterdepolarizations and sustained triggered activity in atrial myocytes. *Am. J. Physiol. Heart Circ. Physiol.* 294:H2031–39
56. Qu Z, Nivala M, Weiss JN. 2013. Calcium alternans in cardiac myocytes: order from disorder. *J. Mol. Cell. Cardiol.* 58:100–9
57. Escobar AL, Valdivia HH. 2014. Cardiac alternans and ventricular fibrillation: a bad case of ryanodine receptors renegeing on their duty. *Circ. Res.* 114:1369–71
58. Eisner DA, Choi HS, Diaz ME, O'Neill SC, Trafford AW. 2000. Integrative analysis of calcium cycling in cardiac muscle. *Circ. Res.* 87:1087–94
59. Shiferaw Y, Watanabe MA, Garfinkel A, Weiss JN, Karma A. 2003. Model of intracellular calcium cycling in ventricular myocytes. *Biophys. J.* 85:3666–86
60. Diaz ME, O'Neill SC, Eisner DA. 2004. Sarcoplasmic reticulum calcium content fluctuation is the key to cardiac alternans. *Circ. Res.* 94:650–56
61. Li Y, Diaz ME, Eisner DA, O'Neill S. 2009. The effects of membrane potential, SR Ca²⁺ content and RyR responsiveness on systolic Ca²⁺ alternans in rat ventricular myocytes. *J. Physiol.* 587:1283–92
62. Xie LH, Sato D, Garfinkel A, Qu Z, Weiss JN. 2008. Intracellular Ca alternans: coordinated regulation by sarcoplasmic reticulum release, uptake, and leak. *Biophys. J.* 95:3100–10
63. Picht E, DeSantiago J, Blatter LA, Bers DM. 2006. Cardiac alternans do not rely on diastolic sarcoplasmic reticulum calcium content fluctuations. *Circ. Res.* 99:740–48
64. Shkryl VM, Maxwell JT, Domeier TL, Blatter LA. 2012. Refractoriness of sarcoplasmic reticulum Ca release determines Ca alternans in atrial myocytes. *Am. J. Physiol. Heart Circ. Physiol.* 302:H2310–20
65. Rovetti R, Cui X, Garfinkel A, Weiss JN, Qu Z. 2010. Spark-induced sparks as a mechanism of intracellular calcium alternans in cardiac myocytes. *Circ. Res.* 106:1582–91
66. Nivala M, Qu Z. 2012. Calcium alternans in a couplon network model of ventricular myocytes: role of sarcoplasmic reticulum load. *Am. J. Physiol. Heart Circ. Physiol.* 303:H341–52
67. Restrepo JG, Weiss JN, Karma A. 2008. Calsequestrin-mediated mechanism for cellular calcium transient alternans. *Biophys. J.* 95:3767–89
68. Pastore JM, Girouard SD, Laurita KR, Akar FG, Rosenbaum DS. 1999. Mechanism linking T-wave alternans to the genesis of cardiac fibrillation. *Circulation* 99:1385–94
69. Hayashi H, Shiferaw Y, Sato D, Nihei M, Lin SF, et al. 2007. Dynamic origin of spatially discordant alternans in cardiac tissue. *Biophys. J.* 92:448–60
70. Mironov S, Jalife J, Tolkacheva EG. 2008. Role of conduction velocity restitution and short-term memory in the development of action potential duration alternans in isolated rabbit hearts. *Circulation* 118:17–25
71. Pu JL, Balser JR, Boyden PA. 1998. Lidocaine action on Na⁺ currents in ventricular myocytes from the epicardial border zone of the infarcted heart. *Circ. Res.* 83:431–40
72. Qu Z, Karagueuzian HS, Garfinkel A, Weiss JN. 2004. Effects of Na⁺ channel and cell coupling abnormalities on vulnerability to reentry: a simulation study. *Am. J. Physiol. Heart Circ. Physiol.* 286:H1310–21
73. Keating MT, Sanguinetti MC. 2001. Molecular and cellular mechanisms of cardiac arrhythmias. *Cell* 104:569–80
74. Liu GX, Choi B-R, Ziv O, Li W, de Lange E, et al. 2012. Differential conditions for early afterdepolarizations and triggered activity in cardiomyocytes derived from transgenic LQT1 and LQT2 rabbits. *J. Physiol.* 590:1171–80
75. Nuss HB, Kaab S, Kass DA, Tomaselli GF, Marban E. 1999. Cellular basis of ventricular arrhythmias and abnormal automaticity in heart failure. *Am. J. Physiol. Heart Circ. Physiol.* 277:H80–91
76. Li GR, Lau CP, Ducharme A, Tardif JC, Nattel S. 2002. Transmural action potential and ionic current remodeling in ventricles of failing canine hearts. *Am. J. Physiol. Heart Circ. Physiol.* 283:H1031–41

77. Damiano BP, Rosen MR. 1984. Effects of pacing on triggered activity induced by early afterdepolarizations. *Circulation* 69:1013–25
78. January CT, Riddle JM. 1989. Early afterdepolarizations: mechanism of induction and block. A role for L-type Ca^{2+} current. *Circ. Res.* 64:977–90
79. January CT, Moscucci A. 1992. Cellular mechanisms of early afterdepolarizations. *Ann. N. Y. Acad. Sci.* 644:23–32
80. Zeng J, Rudy Y. 1995. Early afterdepolarizations in cardiac myocytes: mechanism and rate dependence. *Biophys. J.* 68:949–64
81. Roden DM. 1998. Taking the “idio” out of “idiosyncratic”: predicting torsades de pointes. *Pacing Clin. Electrophysiol.* 21:1029–34
82. Qu Z, Xie L-H, Olcese R, Karagueuzian HS, Chen P-S, et al. 2013. Early afterdepolarizations in cardiac myocytes: beyond reduced repolarization reserve. *Cardiovasc. Res.* 99:6–15
83. Volders PG, Vos MA, Szabo B, Sipido KR, de Groot SH, et al. 2000. Progress in the understanding of cardiac early afterdepolarizations and torsades de pointes: time to revise current concepts. *Cardiovasc. Res.* 46:376–92
84. Zhao Z, Wen H, Fefelova N, Allen C, Baba A, et al. 2012. Revisiting the ionic mechanisms of early afterdepolarizations in cardiomyocytes: predominant by Ca waves or Ca currents? *Am. J. Physiol. Heart Circ. Physiol.* 302:H1636–44
85. Burashnikov A, Antzelevitch C. 2003. Reinduction of atrial fibrillation immediately after termination of the arrhythmia is mediated by late phase 3 early afterdepolarization-induced triggered activity. *Circulation* 107:2355–60
86. Maruyama M, Ai T, Chua S-K, Park H-W, Lee Y-S, et al. 2014. Hypokalemia promotes late phase 3 early afterdepolarization and recurrent ventricular fibrillation during isoproterenol infusion in Langendorff perfused rabbit ventricles. *Heart Rhythm* 11:697–706
87. Yeh YH, Wakili R, Qi XY, Chartier D, Boknik P, et al. 2008. Calcium-handling abnormalities underlying atrial arrhythmogenesis and contractile dysfunction in dogs with congestive heart failure. *Circ. Arrhythm. Electrophysiol.* 1:93–102
88. ter Keurs HEDJ, Boyden PA. 2007. Calcium and arrhythmogenesis. *Physiol. Rev.* 87:457–506
89. Xie L-H, Chen F, Karagueuzian HS, Weiss JN. 2009. Oxidative stress-induced afterdepolarizations and calmodulin kinase II signaling. *Circ. Res.* 104:79–86
90. Maruyama M, Joung B, Tang L, Shinohara T, On YK, et al. 2010. Diastolic intracellular calcium-membrane voltage coupling gain and postshock arrhythmias: role of Purkinje fibers and triggered activity. *Circ. Res.* 106:399–408
91. Pogwizd SM, Schlotthauer K, Li L, Yuan W, Bers DM. 2001. Arrhythmogenesis and contractile dysfunction in heart failure: roles of sodium-calcium exchange, inward rectifier potassium current, and residual β -adrenergic responsiveness. *Circ. Res.* 88:1159–67
92. Pogwizd SM, Bers DM. 2002. Calcium cycling in heart failure: the arrhythmia connection. *J. Cardiovasc. Electrophysiol.* 13:88–91
93. Hilliard FA, Steele DS, Laver D, Yang Z, Le Marchand SJ, et al. 2010. Flecainide inhibits arrhythmogenic Ca^{2+} waves by open state block of ryanodine receptor Ca^{2+} release channels and reduction of Ca^{2+} spark mass. *J. Mol. Cell. Cardiol.* 48:293–301
94. Lehnart SE, Mongillo M, Bellinger A, Lindegger N, Chen BX, et al. 2008. Leaky Ca^{2+} release channel/ryanodine receptor 2 causes seizures and sudden cardiac death in mice. *J. Clin. Investig.* 118:2230–45
95. Jiang D, Xiao B, Yang D, Wang R, Choi P, et al. 2004. RyR2 mutations linked to ventricular tachycardia and sudden death reduce the threshold for store-overload-induced Ca^{2+} release (SOICR). *PNAS* 101:13062–67
96. Dirksen WP, Lacombe VA, Chi M, Kalyanasundaram A, Viatchenko-Karpinski S, et al. 2007. A mutation in calsequestrin, CASQ2D307H, impairs sarcoplasmic reticulum Ca^{2+} handling and causes complex ventricular arrhythmias in mice. *Cardiovasc. Res.* 75:69–78
97. Nivala M, Ko CY, Nivala M, Weiss JN, Qu Z. 2012. Criticality in intracellular calcium signaling in cardiac myocytes. *Biophys. J.* 102:2433–42
98. Nivala M, Ko CY, Nivala M, Weiss JN, Qu Z. 2013. The emergence of subcellular pacemaker sites for calcium waves and oscillations. *J. Physiol.* 591:5305–20

99. Rosen MR, Wit AL, Hoffman BF. 1975. Electrophysiology and pharmacology of cardiac arrhythmias. IV. Cardiac antiarrhythmic and toxic effects of digitalis. *Am. Heart J.* 89:391-99
100. Surawicz B. 1998. U wave: facts, hypotheses, misconceptions, and misnomers. *J. Cardiovasc. Electrophysiol.* 9:1117-28
101. di Bernardo D, Murray A. 2002. Origin on the electrocardiogram of U-waves and abnormal U-wave inversion. *Cardiovasc. Res.* 53:202-8
102. Fujiwara K, Tanaka H, Mani H, Nakagami T, Takamatsu T. 2008. Burst emergence of intracellular Ca^{2+} waves evokes arrhythmogenic oscillatory depolarization via the Na^{+} - Ca^{2+} exchanger: simultaneous confocal recording of membrane potential and intracellular Ca^{2+} in the heart. *Circ. Res.* 103:509-18
103. Wasserstrom JA, Shiferaw Y, Chen W, Ramakrishna S, Patel H, et al. 2010. Variability in timing of spontaneous calcium release in the intact rat heart is determined by the time course of sarcoplasmic reticulum calcium load. *Circ. Res.* 107:1117-26
104. Di Diego JM, Sun ZQ, Antzelevitch C. 1996. $I(\text{to})$ and action potential notch are smaller in left versus right canine ventricular epicardium. *Am. J. Physiol. Heart Circ. Physiol.* 271:H548-61
105. Greenstein JL, Wu R, Po S, Tomaselli GF, Winslow RL. 2000. Role of the calcium-independent transient outward current I_{to1} in shaping action potential morphology and duration. *Circ. Res.* 87:1026-33
106. Maoz A, Krogh-Madsen T, Christini DJ. 2009. Instability in action potential morphology underlies phase 2 reentry: a mathematical modeling study. *Heart Rhythm* 6:813-22
107. Cantalapiedra IR, Penaranda A, Mont L, Brugada J, Echebarria B. 2009. Reexcitation mechanisms in epicardial tissue: role of I_{to} density heterogeneities and I_{Na} inactivation kinetics. *J. Theor. Biol.* 259:850-59
108. Miyoshi S, Mitamura H, Fujikura K, Fukuda Y, Tanimoto K, et al. 2003. A mathematical model of phase 2 reentry: role of L-type Ca current. *Am. J. Physiol. Heart Circ. Physiol.* 284:H1285-94
109. Di Diego JM, Antzelevitch C. 1994. High $[\text{Ca}^{2+}]_{\text{o}}$ -induced electrical heterogeneity and extrasystolic activity in isolated canine ventricular epicardium. Phase 2 reentry. *Circulation* 89:1839-50
110. Antzelevitch C. 1999. Ion channels and ventricular arrhythmias: cellular and ionic mechanisms underlying the Brugada syndrome. *Curr. Opin. Cardiol.* 14:274-79
111. Coronel R, Casini S, Koopmann TT, Wilms-Schopman FJG, Verkerk AO, et al. 2005. Right ventricular fibrosis and conduction delay in a patient with clinical signs of Brugada syndrome: a combined electrophysiological, genetic, histopathologic, and computational study. *Circulation* 112:2769-77
112. Scherf D. 1947. Studies on auricular tachycardia caused by aconitine administration. *Proc. Soc. Exp. Biol. Med.* 64:839-44
113. Silva J, Rudy Y. 2003. Mechanism of pacemaking in I_{K1} -downregulated myocytes. *Circ. Res.* 92:261-63
114. Miragoli M, Salvarani N, Rohr S. 2007. Myofibroblasts induce ectopic activity in cardiac tissue. *Circ. Res.* 101:755-58
115. Lakatta EG, Maltsev VA, Vinogradova TM. 2010. A coupled system of intracellular Ca^{2+} clocks and surface membrane voltage clocks controls the timekeeping mechanism of the heart's pacemaker. *Circ. Res.* 106:659-73
116. Nguyen TP, Xie Y, Garfinkel A, Qu Z, Weiss JN. 2012. Arrhythmogenic consequences of myofibroblast-myocyte coupling. *Cardiovasc. Res.* 93:242-51
117. Xie Y, Garfinkel A, Weiss JN, Qu Z. 2009. Cardiac alternans induced by fibroblast-myocyte coupling: mechanistic insights from computational models. *Am. J. Physiol. Heart Circ. Physiol.* 297:H775-84
118. Keener JP. 2003. Model for the onset of fibrillation following coronary artery occlusion. *J. Cardiovasc. Electrophysiol.* 14:1225-32
119. Pinto JM, Boyden PA. 1999. Electrical remodeling in ischemia and infarction. *Cardiovasc. Res.* 42:284-97
120. Madhvari RV, Xie Y, Pantazis A, Garfinkel A, Qu Z, et al. 2011. Shaping a new Ca^{2+} conductance to suppress early afterdepolarizations in cardiac myocytes. *J. Physiol.* 589:6081-92
121. Nerbonne JM. 2000. Molecular basis of functional voltage-gated K^{+} channel diversity in the mammalian myocardium. *J. Physiol.* 525(Part 2):285-98
122. Tuteja D, Xu D, Timofeyev V, Lu L, Sharma D, et al. 2005. Differential expression of small-conductance Ca^{2+} -activated K^{+} channels SK1, SK2, and SK3 in mouse atrial and ventricular myocytes. *Am. J. Physiol. Heart Circ. Physiol.* 289:H2714-23

123. Chua SK, Chang PC, Maruyama M, Turker I, Shinohara T, et al. 2011. Small-conductance calcium-activated potassium channel and recurrent ventricular fibrillation in failing rabbit ventricles. *Circ. Res.* 108:971–79
124. Chang P-C, Hsieh Y-C, Hsueh C-H, Weiss JN, Lin S-F, Chen P-S. 2013. Apamin induces early afterdepolarizations and torsades de pointes ventricular arrhythmia from failing rabbit ventricles exhibiting secondary rises in intracellular calcium. *Heart Rhythm* 10:1516–24
125. Zhao Z, Xie Y, Wen H, Xiao D, Allen C, et al. 2012. Role of the transient outward potassium current in the genesis of early afterdepolarizations in cardiac cells. *Cardiovasc. Res.* 95:308–16
126. Kaufman ES. 2009. Mechanisms and clinical management of inherited channelopathies: long QT syndrome, Brugada syndrome, catecholaminergic polymorphic ventricular tachycardia, and short QT syndrome. *Heart Rhythm* 6:S51–55
127. Akar FG, Aon MA, Tomaselli GF, O'Rourke B. 2005. The mitochondrial origin of postischemic arrhythmias. *J. Clin. Investig.* 115:3527–35
128. Tang L, Joung B, Ogawa M, Chen P-S, Lin S-F. 2012. Intracellular calcium dynamics, shortened action potential duration, and late-phase 3 early afterdepolarization in Langendorff-perfused rabbit ventricles. *J. Cardiovasc. Electrophysiol.* 23:1364–71
129. Sugai Y, Miura M, Hirose M, Wakayama Y, Endoh H, et al. 2009. Contribution of $\text{Na}^+/\text{Ca}^{2+}$ exchange current to the formation of delayed afterdepolarizations in intact rat ventricular muscle. *J. Cardiovasc. Pharmacol.* 53:517–22
130. Rosen M, Danilo P Jr. 1980. Digitalis-induced delayed afterdepolarizations. In *The Slow Inward Current and Cardiac Arrhythmias*, ed. D Zipes, J Bailey, V Elharrar, pp. 417–35. Dordrecht, Neth.: Springer
131. Verkerk AO, Tan HL, Kirkels JH, Ravesloot JH. 2003. Role of Ca^{2+} -activated Cl^- current during proarrhythmic early afterdepolarizations in sheep and human ventricular myocytes. *Acta Physiol. Scand.* 179:143–48
132. Reed A, Kohl P, Peyronnet R. 2014. Molecular candidates for cardiac stretch-activated ion channels. *Glob. Cardiol. Sci. Pract.* 2014:19
133. Bers DM. 2008. Calcium cycling and signaling in cardiac myocytes. *Annu. Rev. Physiol.* 70:23–49
134. Cheng H, Lederer WJ. 2008. Calcium sparks. *Physiol. Rev.* 88:1491–545
135. Stern MD, Rios E, Maltsev VA. 2013. Life and death of a cardiac calcium spark. *J. Gen. Physiol.* 142:257–74
136. Sobie EA, Song LS, Lederer WJ. 2006. Restitution of Ca^{2+} release and vulnerability to arrhythmias. *J. Cardiovasc. Electrophysiol.* 17(Suppl. 1):64–70
137. Winslow RL, Greenstein JL. 2013. Extinguishing the sparks. *Biophys. J.* 104:2115–17
138. Gaeta SA, Bub G, Abbott GW, Christini DJ. 2009. Dynamical mechanism for subcellular alternans in cardiac myocytes. *Circ. Res.* 105:335–42
139. Tian Q, Kaestner L, Lipp P. 2012. Noise-free visualization of microscopic calcium signaling by pixel-wise fitting. *Circ. Res.* 111:17–27
140. Cheng H, Lederer MR, Lederer WJ, Cannell MB. 1996. Calcium sparks and $[\text{Ca}^{2+}]_i$ waves in cardiac myocytes. *Am. J. Physiol. Cell Physiol.* 270:C148–59
141. Wier WG, ter Keurs HE, Marban E, Gao WD, Balke CW. 1997. Ca^{2+} “sparks” and waves in intact ventricular muscle resolved by confocal imaging. *Circ. Res.* 81:462–69
142. Belevych AE, Terentyev D, Terentyeva R, Ho HT, Gyorke I, et al. 2012. Shortened Ca^{2+} signaling refractoriness underlies cellular arrhythmogenesis in a postinfarction model of sudden cardiac death. *Circ. Res.* 110:569–77
143. O'Rourke B, Maack C. 2007. The role of Na dysregulation in cardiac disease and how it impacts electrophysiology. *Drug Discov. Today Dis. Models* 4:207–17
144. Webster G, Berul CI. 2013. An update on channelopathies: from mechanisms to management. *Circulation* 127:126–40
145. Clancy CE, Rudy Y. 2002. Na^+ channel mutation that causes both Brugada and long-QT syndrome phenotypes: a simulation study of mechanism. *Circulation* 105:1208–13
146. Wagner S, Rokita AG, Anderson ME, Maier LS. 2013. Redox regulation of sodium and calcium handling. *Antioxid. Redox Signal.* 18:1063–77

147. Dobrev D, Wehrens XHT. 2014. Role of RyR2 phosphorylation in heart failure and arrhythmias: controversies around ryanodine receptor phosphorylation in cardiac disease. *Circ. Res.* 114:1311–19
148. Jeong E-M, Liu M, Sturdy M, Gao G, Varghese ST, et al. 2012. Metabolic stress, reactive oxygen species, and arrhythmia. *J. Mol. Cell. Cardiol.* 52:454–63
149. Swaminathan PD, Purohit A, Hund TJ, Anderson ME. 2012. Calmodulin-dependent protein kinase II: linking heart failure and arrhythmias. *Circ. Res.* 110:1661–77
150. Boyden PA, Dun W, Barbhaiya C, Ter Keurs HE. 2004. 2APB- and JTV519(K201)-sensitive micro Ca^{2+} waves in arrhythmogenic Purkinje cells that survive in infarcted canine heart. *Heart Rhythm* 1:218–26
151. Lipp P, Niggli E. 1993. Microscopic spiral waves reveal positive feedback in subcellular calcium signaling. *Biophys. J.* 65:2272–76
152. Xie F, Qu Z, Yang J, Baher A, Weiss JN, Garfinkel A. 2004. A simulation study of the effects of cardiac anatomy in ventricular fibrillation. *J. Clin. Investig.* 113:686–93



Contents

PERSPECTIVES, *David Julius, Editor*

A Conversation with Oliver Smithies <i>Oliver Smithies and Tom Coffman</i>	1
---	---

CARDIOVASCULAR PHYSIOLOGY, *Marlene Rabinovitch, Section Editor*

Exosomes: Vehicles of Intercellular Signaling, Biomarkers, and Vectors of Cell Therapy <i>Stella Kourembanas</i>	13
--	----

Mechanisms of Ventricular Arrhythmias: From Molecular Fluctuations to Electrical Turbulence <i>Zhilin Qu and James N. Weiss</i>	29
---	----

CELL PHYSIOLOGY, *David E. Clapham, Section Editor*

Lysosomal Physiology <i>Haoxing Xu and Dejian Ren</i>	57
--	----

Phosphoinositide Control of Membrane Protein Function: A Frontier Led by Studies on Ion Channels <i>Diomedes E. Logothetis, Vasileios I. Petrou, Miao Zhang, Rabul Mahajan, Xuan-Yu Meng, Scott K. Adney, Meng Cui, and Lia Baki</i>	81
--	----

ENDOCRINOLOGY, *Holly A. Ingraham, Section Editor*

Hedgehog Signaling and Steroidogenesis <i>Isabella Finco, Christopher R. LaPensee, Kenneth T. Krill, and Gary D. Hammer</i>	105
--	-----

Hypothalamic Inflammation in the Control of Metabolic Function <i>Martin Valdearcos, Allison W. Xu, and Suneil K. Koliwad</i>	131
--	-----

Regulation of Body Fat in <i>Caenorhabditis elegans</i> <i>Supriya Srinivasan</i>	161
--	-----

GASTROINTESTINAL PHYSIOLOGY, Linda Samuelson, Section Editor

Cellular Homeostasis and Repair in the Mammalian Liver
Ben Z. Stanger 179

Hippo Pathway Regulation of Gastrointestinal Tissues
Fa-Xing Yu, Zhipeng Meng, Steven W. Plouffe, and Kun-Liang Guan 201

Regeneration and Repair of the Exocrine Pancreas
L. Charles Murtaugh and Matthew D. Keefe 229

NEUROPHYSIOLOGY, Roger Nicoll, Section Editor

Homeostatic Control of Presynaptic Neurotransmitter Release
Graeme W. Davis and Martin Müller 251

Intrinsic and Extrinsic Mechanisms of Dendritic Morphogenesis
Xintong Dong, Kang Shen, and Hannes E. Bülow 271

RENAL AND ELECTROLYTE PHYSIOLOGY, Peter Aronson, Section Editor

Concurrent Activation of Multiple Vasoactive Signaling Pathways
in Vasoconstriction Caused by Tubuloglomerular Feedback:
A Quantitative Assessment
Jurgen Schnermann 301

The Molecular Physiology of Uric Acid Homeostasis
Asim K. Mandal and David B. Mount 323

Physiological Roles of Acid-Base Sensors
Lonnie R. Levin and Jochem Buck 347

The Role of Pendrin in Renal Physiology
Susan M. Wall and Yoskaly Lazo-Fernandez 363

RESPIRATORY PHYSIOLOGY, Augustine M.K. Choi, Section Editor

Cilia Dysfunction in Lung Disease
Ann E. Tilley, Matthew S. Walters, Renat Shaykhiev, and Ronald G. Crystal 379

Dynamics of Lung Defense in Pneumonia: Resistance, Resilience,
and Remodeling
Lee J. Quinton and Joseph P. Mizgerd 407

Nitrogen Chemistry and Lung Physiology
Nadzeya V. Marozkina and Benjamin Gaston 431

Unmasking the Lung Cancer Epigenome
Steven A. Belinsky 453

SPECIAL TOPIC: GENETIC AND MOLECULAR BASIS OF EPISODIC DISORDERS, *Louis J. Ptáček, Section Editor*

Episodic Disorders: Channelopathies and Beyond
Louis J. Ptáček 475

Sodium Channel β Subunits: Emerging Targets in Channelopathies
Heather A. O'Malley and Lori L. Isom 481

Alternative Paradigms for Ion Channelopathies: Disorders of Ion Channel Membrane Trafficking and Posttranslational Modification
Jerry Curran and Peter J. Mobler 505

Episodic and Electrical Nervous System Disorders Caused by Nonchannel Genes
Hsien-yang Lee, Ying-Hui Fu, and Louis J. Ptáček 525

Indexes

Cumulative Index of Contributing Authors, Volumes 73–77 000

Cumulative Index of Article Titles, Volumes 73–77 000

Errata

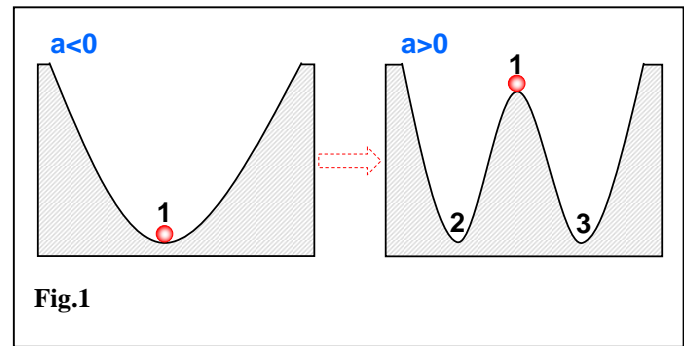
An online log of corrections to *Annual Review of Physiology* articles may be found at <http://www.annualreviews.org/errata/physiol>

Supplemental text

1. Equilibrium point, dynamic instabilities and bifurcation

An equilibrium is a state of a system at which the positive and negative forces are balanced. In nonlinear dynamics, an equilibrium point is also called a steady state or a fixed point. The resting potential of a ventricular myocyte is an equilibrium point at which inward current equals to outward current. The plateau of a ventricular action potential is a quasi-equilibrium state especially when the action potential is very long, at which the inward and outward currents are approximately equal with slightly larger outward current which eventually repolarizes the cell. If there is enough steady state inward current, such as late I_{Na} or window and pedestal $I_{Ca,L}$, the plateau can become a true equilibrium, which has been observed experimentally (2). When a ventricular myocyte is subjected to periodic pacing at a slow pacing rate, it reaches a steady state in which the APD and DI become constant from beat to beat. This is also an equilibrium state.

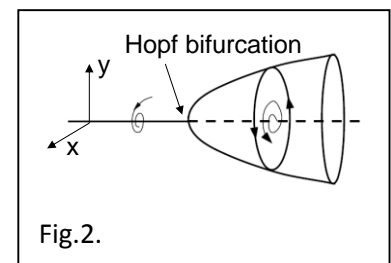
An equilibrium can be stable or become unstable. For example, the potential described by $V(x) = -ax^2 + bx^4$, is a single-well potential when the parameter $a < 0$, with the equilibrium point at $x=0$, which is at the minimum potential and thus *stable* (Fig.1). However, if the parameter a changes from negative to positive, i.e., $a > 0$, the single-well potential becomes a double-well potential. $x=0$ is still an equilibrium point and two new equilibrium points emerge. But now $x=0$ is a maximum of the potential and thus it becomes *unstable* since any small perturbation will lead the system to either state 2 or 3. The two new equilibrium points, 2 and 3, are at the valleys of the potential and thus are stable equilibrium points. Since the system has two stable equilibrium points for the same parameter a , it is called *bistable*. The experimental observation by Gadsby and Cranefield (2) that two resting potentials exist at the same cell is a bistable behavior. *Bi-excitability* reviewed in the present article is also a bistable behavior.



$a=0$ is the parameter point at which the system undergoes the aforementioned qualitative change, which is called a *bifurcation* point. The qualitative change in behavior of the equilibrium point of a nonlinear system is thus caused by a *dynamic instability*. An equilibrium can lose its stability via different ways (aka different dynamic instabilities) depending on the properties of the nonlinear system (3), resulting in different types of bifurcations and thus leading the system to different behaviors, such as oscillations and chaos. In cardiac systems, APD and Ca^{2+} alternans, EADs, and automaticity are resulted from bifurcations due to loss of stability of the equilibrium state, or caused by dynamic instabilities.

2. Hopf bifurcation

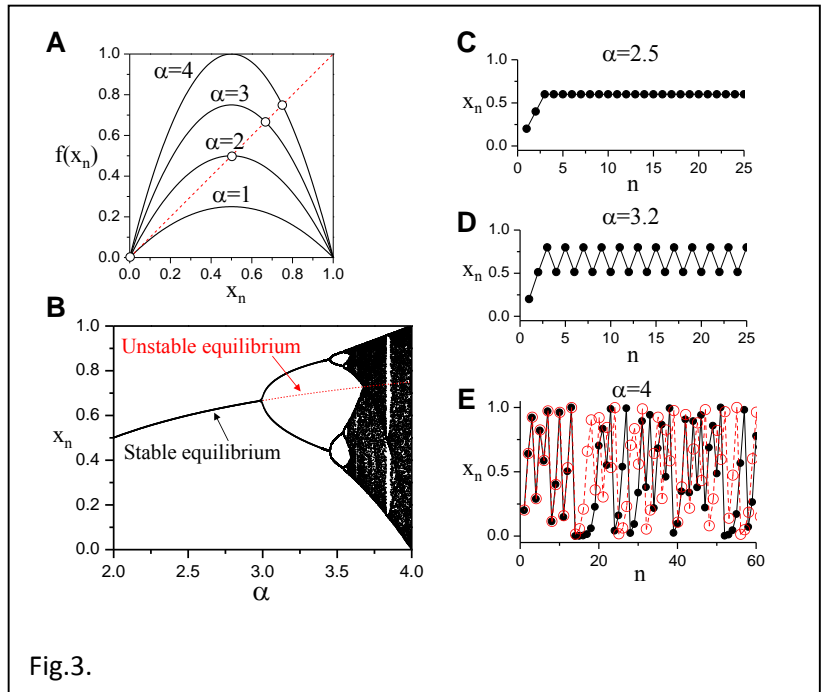
Hopf bifurcation is a type of bifurcation that leads to oscillations in a nonlinear system (Fig.2). Before the bifurcation point, a transient oscillation occurs if the system displaced from the equilibrium state, but the system returns to the equilibrium state. After the bifurcation point, the equilibrium is unstable, and the system will enter an oscillatory state, called a limit cycle. The key biological processes causing oscillatory behavior are positive feedback and/or negative feedback with steeply-sloped functions (4, 5). The positive feedback tends to pull the system away from the equilibrium, while the negative feedback tends to return it to equilibrium. When the functions involved (such as the steady-state activation and inactivation curves of an ion channel) are steep and the positive feedback is much faster than the negative feedback, oscillations develop. For example, the resting membrane potential of a ventricular myocyte can become unstable via a Hopf bifurcation in response to the drug aconitine which blocks the Na^+ channel inactivation (6), or if I_{K1} is blocked (7),



leading to oscillations (pacemaking). Under the conditions of reduced repolarization reserve, when the quasi-equilibrium state during the plateau of a ventricular action potential becomes unstable via the Hopf bifurcation, voltage oscillations occur, leading to EADs (8). When the quasi-equilibrium is stable, an ultralong action potential is resulted (9). Whether the quasi-equilibrium is stable or not depends on the time constants and the slopes of the steady-state curves of activation and inactivation of L-type Ca current and those of other currents influencing repolarization and depolarization (8-10).

3. Chaos

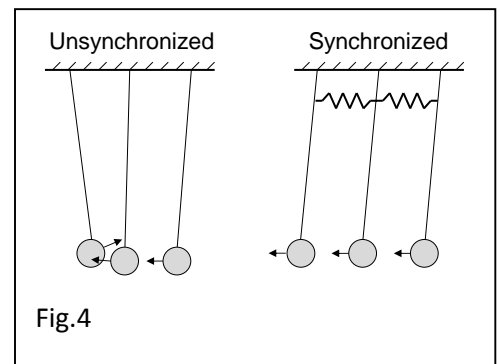
Chaos is a complex irregular behavior arising from deterministic nonlinear systems under certain parameter settings, which looks erratic and random but is not truly random. Chaos can be generated from very simple systems. Such a text book example is the so-called Logistic map (3, 11): $x_{n+1} = f(x_n) = ax_n(1 - x_n)$, which is also the equation for a parabola. The map: $APD_{n+1} = f(DI_n) = f(CL - APD_n)$, which is widely used to study APD alternans and chaos, is the same type of iterated map as the Logistic map. $f(x_n)$ in the Logistic map is a parabolic function (Fig.3A). The equilibrium states are the solutions of the equation $x_n=f(x_n)$, which are simply the intersections of the parabolae and the diagonal line (Fig.3A). The behaviors of the Logistic map are summarized in the bifurcation diagram shown in Fig.3B, in which the steady state values of x_n (after the initial transients have disappeared) versus the parameter a are plotted. When $a < 3$, the non-zero equilibrium state is stable, and the system always approaches this equilibrium state with any initial conditions (Fig.1C). However, as a increases beyond 3, the equilibrium state becomes unstable (dashed line in Fig.3B), and a new type of behavior emerges, which exhibits a large-small-large-small alternating pattern (Fig.3D). This is the same bifurcation that leads to APD alternans in a cardiac myocyte. Note that the slope of $f(x_n)$ at the equilibrium point becomes steeper as a increases (see Fig.3A), which causes the equilibrium state to be unstable when $a > 3$. As a increases further, more complex behaviors occur, and eventually x_n behaves in a non-periodic manner (Fig.3E), which is dynamical chaos.



Chaos is qualitatively different from the periodic behaviors, not only due to its erratic appearance but also due to its sensitivity to initial perturbations. For example, the two chaotic traces shown in Fig.3E are results from two different initial conditions: $x_1=0.2$ and $x_1=0.20001$. Although the initial difference is only 10^{-5} , it gets amplified after about 10 iterations to the macroscopic scale that makes the two iteration sequences to look completely different. This property is the hallmark of chaos: sensitive dependence on initial conditions, also called the “butterfly effect” (12, 13). If two myocytes behave chaotically, and if they are not coupled, their beat-to-beat action potentials will look completely different.

Chaos has been shown in cardiac myocytes in many studies (14-17) and can theoretically studied using the APD restitution map (18).

4. Synchronization



Synchronization refers to oscillators that oscillate exactly in-phase. For example, uncoupled pendulums oscillate out-of-phase due to initial phase difference and their slightly different frequencies. However, when they are coupled, even weakly, they can become exactly synchronized (Fig.4). If they are identical periodic oscillators, a weak coupling is enough to cause them to synchronize. However, if they are identical chaotic oscillators, they can still be synchronized, but synchronization depends on the coupling strength and the number of oscillators coupled (19, 20). When the coupling is too weak or too many oscillators are coupled, synchronization fails, however, the neighboring oscillators still oscillate roughly in-phase but distant ones will be out-of-phase. The reason that chaotic oscillators tend to desynchronize is due to the “butterfly effect”. In cardiac tissue, loss of synchronization of cardiac myocytes due to chaos can result in large dispersion of refractoriness to form reentry substrates and triggers, and lead to multiple shifting focal excitations (17, 21).

5. Criticality

Criticality is a universal phenomenon of thermodynamic systems (22), which occurs during second-order phase transitions. At the point, certain quantities in the system, for example specific heat, diverge. When a system reaches criticality, it contains all sizes of length scales which exhibit a power-law distribution (Fig.5). Later studies have shown that the ubiquitous behavior of power-law distribution in nature is a result of so-called self-organized criticality (23). The transitions from Ca sparks to Ca waves is governed by the same critical dynamics in which the sparks cluster exhibit a power-law (24). When a system is in criticality, a small perturbation may result in a large-scale crisis, such as in snow avalanches and earthquakes (25).

6. Basins of attraction

When a system has only one stable solution, the system will always approach this state starting from any initial state, such as in Fig.1A. In nonlinear systems, however, there can be more than one stable solution for the same set of parameters, such as bistability in Fig.1B. When a system has multiple stable solutions, the initial state determines the final state of the system. The basin of attraction of a solution is the range of the initial states that lead the system to the solution. For the double-well potential shown in Fig.1B, any initial state at the left side of “1” leads the system to solution 2 and any initial state at the right side of “1” leads the system to solution 3. The basin of attraction of a solution in high-dimensional nonlinear system can be very complicated (26). A normal heart can be in either sinus rhythm or fibrillation. However, to cause a normal heart to fibrillate requires a large electrical shock to displace it from the sinus rhythm basin of attraction to the fibrillation basin of attraction. Fortunately, sinus rhythm has a large basin of attraction so that small perturbations like spontaneous PVCs stand virtually no chance of inducing fibrillation. But in diseased heart, it is much easier to induce fibrillation, indicating that the basin of attraction of the sinus rhythm is reduced or that of fibrillation has increased.

References:

1. Jung P, Cornell-Bell A, Madden KS, Moss F. 1998. Noise-induced spiral waves in astrocyte syncytia show evidence of self-organized criticality. *J Neurophysiol* 79: 1098-101
2. Gadsby DC, Cranefield PF. 1977. Two levels of resting potential in cardiac Purkinje fibers. *J Gen Physiol* 70: 725-46

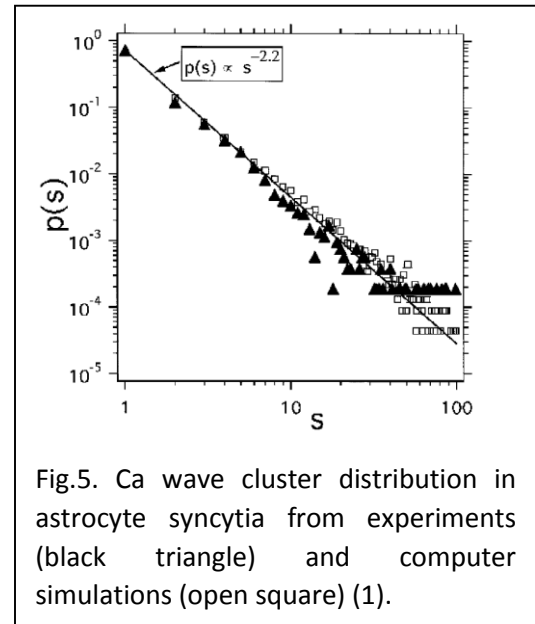


Fig.5. Ca wave cluster distribution in astrocyte syncytia from experiments (black triangle) and computer simulations (open square) (1).

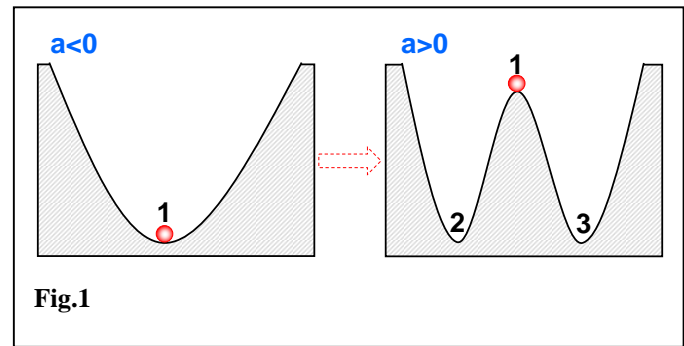
3. Strogatz SH. 2000. *Nonlinear dynamics and Chaos: with applications to physics, biology, chemistry, and engineering*. Cambridge: Westview Press. xi, 498 pp.
4. Tyson JJ. 2002. Biochemical oscillations. In *Computational Cell Biology*, ed. CP Fall, ES Marland, JM Wagner, JJ Tyson, pp. 230-60. New York, Berlin: Springer
5. Qu Z, Weiss JN, MacLellan WR. 2003. Regulation of the mammalian cell cycle: a model of the G1-to-S transition. *Am J Physiol Cell Physiol* 284: C349-64.
6. Scherf D. 1947. Studies on auricular tachycardia caused by aconitine administration. *Proc Soc Exp Biol Med* 64: 839-44
7. Silva J, Rudy Y. 2003. Mechanism of Pacemaking in IK1-Downregulated Myocytes. *Circulation Research* 92: 261-63
8. Tran DX, Sato D, Yochelis A, Weiss JN, Garfinkel A, Qu Z. 2009. Bifurcation and Chaos in a Model of Cardiac Early Afterdepolarizations. *Physical Review Letters* 102: 258103
9. Qu Z, Chung D. 2012. Mechanisms and determinants of ultralong action potential duration and slow rate-dependence in cardiac myocytes. *PLoS One* 7: e43587
10. Qu Z, Xie L-H, Olcese R, Karagueuzian HS, Chen P-S, et al. 2013. Early afterdepolarizations in cardiac myocytes: beyond reduced repolarization reserve. *Cardiovascular Research* 99: 6-15
11. May RM. 1976. Simple mathematical models with very complicated dynamics. *Nature* 261: 459-67
12. Lorenz EN. 1994. *The Essence of Chaos*. Seattle: University of Washington Press
13. Hilborn RC. 2004. Sea gulls, butterflies, and grasshoppers: A brief history of the butterfly effect in nonlinear dynamics. *Am J Phys* 72: 425-27
14. Chialvo DR, Gilmour RF, Jalife J. 1990. Low dimensional chaos in cardiac tissue. *Nature* 343: 653-57
15. Watanabe M, Otani NF, Gilmour RF. 1995. Biphasic restitution of action potential duration and complex dynamics in ventricular myocardium. *Circ. Res.* 76: 915-21
16. Sato D, Xie LH, Nguyen TP, Weiss JN, Qu Z. 2010. Irregularly appearing early afterdepolarizations in cardiac myocytes: random fluctuations or dynamical chaos? *Biophys J* 99: 765-73
17. Sato D, Xie LH, Sovari AA, Tran DX, Morita N, et al. 2009. Synchronization of chaotic early afterdepolarizations in the genesis of cardiac arrhythmias. *Proc Natl Acad Sci U S A* 106: 2983-8
18. Qu Z, Shiferaw Y, Weiss JN. 2007. Nonlinear dynamics of cardiac excitation-contraction coupling: an iterated map study. *Phys Rev E* 75: 011927
19. Pecora LM, Carroll TL. 1990. Synchronization in chaotic systems. *Physical Review Letters* 64: 821-24
20. Heagy JF, Carroll TL, Pecora LM. 1994. Synchronous chaos in coupled oscillator systems. *Physical Review E* 50: 1874-85
21. Xie Y, Hu G, Sato D, Weiss JN, Garfinkel A, Qu Z. 2007. Dispersion of refractoriness and induction of reentry due to chaos synchronization in a model of cardiac tissue. *Phys. Rev. Lett.* 99: 118101
22. Stanley HE. 1999. Scaling, universality, and renormalization: Three pillars of modern critical phenomena. *Rev. Mod. Phys.* 71: S358-S66
23. Bak P, Tang C, Wiesenfeld K. 1988. Self-organized criticality. *Phys Rev A* 38: 364-74
24. Nivala M, Ko CY, Nivala M, Weiss JN, Qu Z. 2012. Criticality in intracellular calcium signaling in cardiac myocytes. *Biophys J* 102: 2433-42
25. Bak P. 1997. *How Nature Works: The Science of Self-Organized Criticality*. New York: Oxford University Press
26. Nusse HE, Yorke JA. 1996. Basins of Attraction. *Science* 271: 1376-80

Supplemental text

1. Equilibrium point, dynamic instabilities and bifurcation

An equilibrium is a state of a system at which the positive and negative forces are balanced. In nonlinear dynamics, an equilibrium point is also called a steady state or a fixed point. The resting potential of a ventricular myocyte is an equilibrium point at which inward current equals to outward current. The plateau of a ventricular action potential is a quasi-equilibrium state especially when the action potential is very long, at which the inward and outward currents are approximately equal with slightly larger outward current which eventually repolarizes the cell. If there is enough steady state inward current, such as late I_{Na} or window and pedestal $I_{Ca,L}$, the plateau can become a true equilibrium, which has been observed experimentally (2). When a ventricular myocyte is subjected to periodic pacing at a slow pacing rate, it reaches a steady state in which the APD and DI become constant from beat to beat. This is also an equilibrium state.

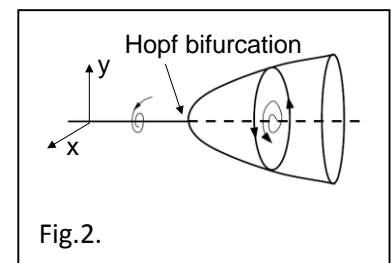
An equilibrium can be stable or become unstable. For example, the potential described by $V(x) = -ax^2 + bx^4$, is a single-well potential when the parameter $a < 0$, with the equilibrium point at $x=0$, which is at the minimum potential and thus *stable* (Fig.1). However, if the parameter a changes from negative to positive, i.e., $a > 0$, the single-well potential becomes a double-well potential. $x=0$ is still an equilibrium point and two new equilibrium points emerge. But now $x=0$ is a maximum of the potential and thus it becomes *unstable* since any small perturbation will lead the system to either state 2 or 3. The two new equilibrium points, 2 and 3, are at the valleys of the potential and thus are stable equilibrium points. Since the system has two stable equilibrium points for the same parameter a , it is called *bistable*. The experimental observation by Gadsby and Cranefield (2) that two resting potentials exist at the same cell is a bistable behavior. *Bi-excitability* reviewed in the present article is also a bistable behavior.



$a=0$ is the parameter point at which the system undergoes the aforementioned qualitative change, which is called a *bifurcation* point. The qualitative change in behavior of the equilibrium point of a nonlinear system is thus caused by a *dynamic instability*. An equilibrium can lose its stability via different ways (aka different dynamic instabilities) depending on the properties of the nonlinear system (3), resulting in different types of bifurcations and thus leading the system to different behaviors, such as oscillations and chaos. In cardiac systems, APD and Ca^{2+} alternans, EADs, and automaticity are resulted from bifurcations due to loss of stability of the equilibrium state, or caused by dynamic instabilities.

2. Hopf bifurcation

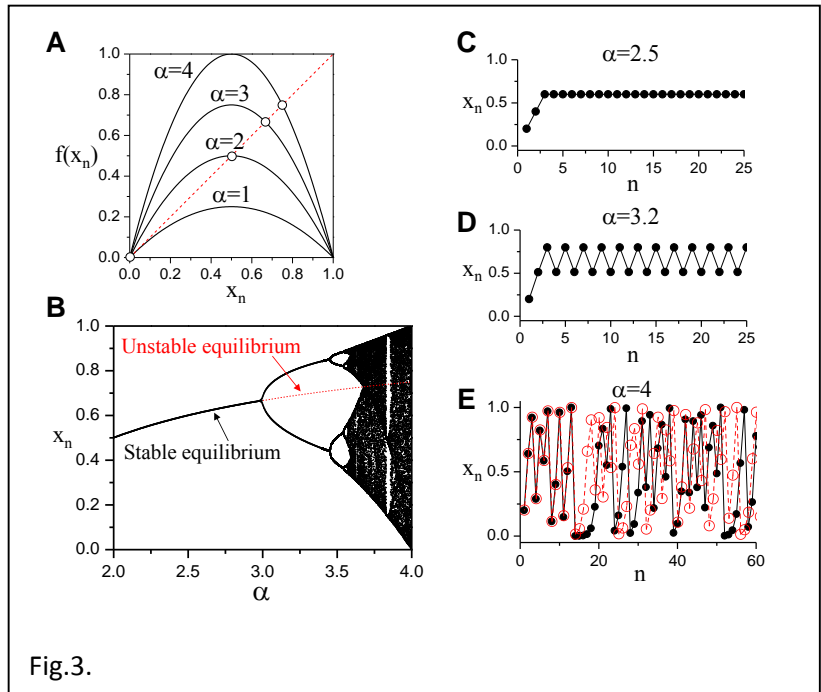
Hopf bifurcation is a type of bifurcation that leads to oscillations in a nonlinear system (Fig.2). Before the bifurcation point, a transient oscillation occurs if the system displaced from the equilibrium state, but the system returns to the equilibrium state. After the bifurcation point, the equilibrium is unstable, and the system will enter an oscillatory state, called a limit cycle. The key biological processes causing oscillatory behavior are positive feedback and/or negative feedback with steeply-sloped functions (4, 5). The positive feedback tends to pull the system away from the equilibrium, while the negative feedback tends to return it to equilibrium. When the functions involved (such as the steady-state activation and inactivation curves of an ion channel) are steep and the positive feedback is much faster than the negative feedback, oscillations develop. For example, the resting membrane potential of a ventricular myocyte can become unstable via a Hopf bifurcation in response to the drug aconitine which blocks the Na^+ channel inactivation (6), or if I_{K1} is blocked (7),



leading to oscillations (pacemaking). Under the conditions of reduced repolarization reserve, when the quasi-equilibrium state during the plateau of a ventricular action potential becomes unstable via the Hopf bifurcation, voltage oscillations occur, leading to EADs (8). When the quasi-equilibrium is stable, an ultralong action potential is resulted (9). Whether the quasi-equilibrium is stable or not depends on the time constants and the slopes of the steady-state curves of activation and inactivation of L-type Ca current and those of other currents influencing repolarization and depolarization (8-10).

3. Chaos

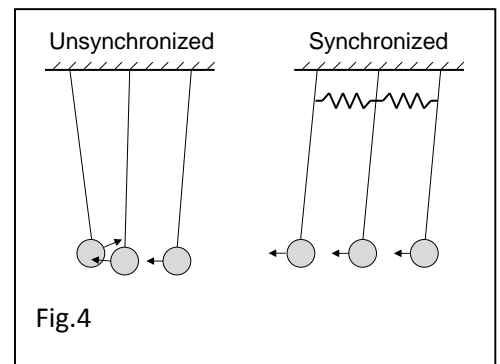
Chaos is a complex irregular behavior arising from deterministic nonlinear systems under certain parameter settings, which looks erratic and random but is not truly random. Chaos can be generated from very simple systems. Such a text book example is the so-called Logistic map (3, 11): $x_{n+1} = f(x_n) = ax_n(1 - x_n)$, which is also the equation for a parabola. The map: $APD_{n+1} = f(DI_n) = f(CL - APD_n)$, which is widely used to study APD alternans and chaos, is the same type of iterated map as the Logistic map. $f(x_n)$ in the Logistic map is a parabolic function (Fig.3A). The equilibrium states are the solutions of the equation $x_n=f(x_n)$, which are simply the intersections of the parabolae and the diagonal line (Fig.3A). The behaviors of the Logistic map are summarized in the bifurcation diagram shown in Fig.3B, in which the steady state values of x_n (after the initial transients have disappeared) versus the parameter a are plotted. When $a < 3$, the non-zero equilibrium state is stable, and the system always approaches this equilibrium state with any initial conditions (Fig.1C). However, as a increases beyond 3, the equilibrium state becomes unstable (dashed line in Fig.3B), and a new type of behavior emerges, which exhibits a large-small-large-small alternating pattern (Fig.3D). This is the same bifurcation that leads to APD alternans in a cardiac myocyte. Note that the slope of $f(x_n)$ at the equilibrium point becomes steeper as a increases (see Fig.3A), which causes the equilibrium state to be unstable when $a > 3$. As a increases further, more complex behaviors occur, and eventually x_n behaves in a non-periodic manner (Fig.3E), which is dynamical chaos.



Chaos is qualitatively different from the periodic behaviors, not only due to its erratic appearance but also due to its sensitivity to initial perturbations. For example, the two chaotic traces shown in Fig.3E are results from two different initial conditions: $x_1=0.2$ and $x_1=0.20001$. Although the initial difference is only 10^{-5} , it gets amplified after about 10 iterations to the macroscopic scale that makes the two iteration sequences to look completely different. This property is the hallmark of chaos: sensitive dependence on initial conditions, also called the “butterfly effect” (12, 13). If two myocytes behave chaotically, and if they are not coupled, their beat-to-beat action potentials will look completely different.

Chaos has been shown in cardiac myocytes in many studies (14-17) and can theoretically studied using the APD restitution map (18).

4. Synchronization



Synchronization refers to oscillators that oscillate exactly in-phase. For example, uncoupled pendulums oscillate out-of-phase due to initial phase difference and their slightly different frequencies. However, when they are coupled, even weakly, they can become exactly synchronized (Fig.4). If they are identical periodic oscillators, a weak coupling is enough to cause them to synchronize. However, if they are identical chaotic oscillators, they can still be synchronized, but synchronization depends on the coupling strength and the number of oscillators coupled (19, 20). When the coupling is too weak or too many oscillators are coupled, synchronization fails, however, the neighboring oscillators still oscillate roughly in-phase but distant ones will be out-of-phase. The reason that chaotic oscillators tend to desynchronize is due to the “butterfly effect”. In cardiac tissue, loss of synchronization of cardiac myocytes due to chaos can result in large dispersion of refractoriness to form reentry substrates and triggers, and lead to multiple shifting focal excitations (17, 21).

5. Criticality

Criticality is a universal phenomenon of thermodynamic systems (22), which occurs during second-order phase transitions. At the point, certain quantities in the system, for example specific heat, diverge. When a system reaches criticality, it contains all sizes of length scales which exhibit a power-law distribution (Fig.5). Later studies have shown that the ubiquitous behavior of power-law distribution in nature is a result of so-called self-organized criticality (23). The transitions from Ca sparks to Ca waves is governed by the same critical dynamics in which the sparks cluster exhibit a power-law (24). When a system is in criticality, a small perturbation may result in a large-scale crisis, such as in snow avalanches and earthquakes (25).

6. Basins of attraction

When a system has only one stable solution, the system will always approach this state starting from any initial state, such as in Fig.1A. In nonlinear systems, however, there can be more than one stable solution for the same set of parameters, such as bistability in Fig.1B. When a system has multiple stable solutions, the initial state determines the final state of the system. The basin of attraction of a solution is the range of the initial states that lead the system to the solution. For the double-well potential shown in Fig.1B, any initial state at the left side of “1” leads the system to solution 2 and any initial state at the right side of “1” leads the system to solution 3. The basin of attraction of a solution in high-dimensional nonlinear system can be very complicated (26). A normal heart can be in either sinus rhythm or fibrillation. However, to cause a normal heart to fibrillate requires a large electrical shock to displace it from the sinus rhythm basin of attraction to the fibrillation basin of attraction. Fortunately, sinus rhythm has a large basin of attraction so that small perturbations like spontaneous PVCs stand virtually no chance of inducing fibrillation. But in diseased heart, it is much easier to induce fibrillation, indicating that the basin of attraction of the sinus rhythm is reduced or that of fibrillation has increased.

References:

1. Jung P, Cornell-Bell A, Madden KS, Moss F. 1998. Noise-induced spiral waves in astrocyte syncytia show evidence of self-organized criticality. *J Neurophysiol* 79: 1098-101
2. Gadsby DC, Cranefield PF. 1977. Two levels of resting potential in cardiac Purkinje fibers. *J Gen Physiol* 70: 725-46

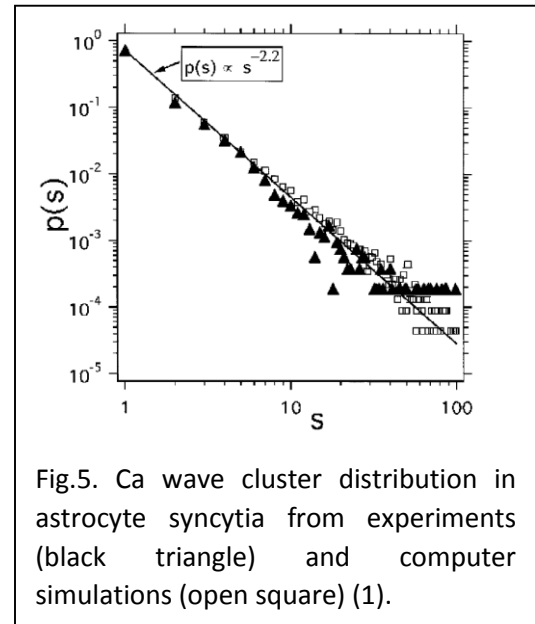


Fig.5. Ca wave cluster distribution in astrocyte syncytia from experiments (black triangle) and computer simulations (open square) (1).

3. Strogatz SH. 2000. *Nonlinear dynamics and Chaos: with applications to physics, biology, chemistry, and engineering*. Cambridge: Westview Press. xi, 498 pp.
4. Tyson JJ. 2002. Biochemical oscillations. In *Computational Cell Biology*, ed. CP Fall, ES Marland, JM Wagner, JJ Tyson, pp. 230-60. New York, Berlin: Springer
5. Qu Z, Weiss JN, MacLellan WR. 2003. Regulation of the mammalian cell cycle: a model of the G1-to-S transition. *Am J Physiol Cell Physiol* 284: C349-64.
6. Scherf D. 1947. Studies on auricular tachycardia caused by aconitine administration. *Proc Soc Exp Biol Med* 64: 839-44
7. Silva J, Rudy Y. 2003. Mechanism of Pacemaking in IK1-Downregulated Myocytes. *Circulation Research* 92: 261-63
8. Tran DX, Sato D, Yochelis A, Weiss JN, Garfinkel A, Qu Z. 2009. Bifurcation and Chaos in a Model of Cardiac Early Afterdepolarizations. *Physical Review Letters* 102: 258103
9. Qu Z, Chung D. 2012. Mechanisms and determinants of ultralong action potential duration and slow rate-dependence in cardiac myocytes. *PLoS One* 7: e43587
10. Qu Z, Xie L-H, Olcese R, Karagueuzian HS, Chen P-S, et al. 2013. Early afterdepolarizations in cardiac myocytes: beyond reduced repolarization reserve. *Cardiovascular Research* 99: 6-15
11. May RM. 1976. Simple mathematical models with very complicated dynamics. *Nature* 261: 459-67
12. Lorenz EN. 1994. *The Essence of Chaos*. Seattle: University of Washington Press
13. Hilborn RC. 2004. Sea gulls, butterflies, and grasshoppers: A brief history of the butterfly effect in nonlinear dynamics. *Am J Phys* 72: 425-27
14. Chialvo DR, Gilmour RF, Jalife J. 1990. Low dimensional chaos in cardiac tissue. *Nature* 343: 653-57
15. Watanabe M, Otani NF, Gilmour RF. 1995. Biphasic restitution of action potential duration and complex dynamics in ventricular myocardium. *Circ. Res.* 76: 915-21
16. Sato D, Xie LH, Nguyen TP, Weiss JN, Qu Z. 2010. Irregularly appearing early afterdepolarizations in cardiac myocytes: random fluctuations or dynamical chaos? *Biophys J* 99: 765-73
17. Sato D, Xie LH, Sovari AA, Tran DX, Morita N, et al. 2009. Synchronization of chaotic early afterdepolarizations in the genesis of cardiac arrhythmias. *Proc Natl Acad Sci U S A* 106: 2983-8
18. Qu Z, Shiferaw Y, Weiss JN. 2007. Nonlinear dynamics of cardiac excitation-contraction coupling: an iterated map study. *Phys Rev E* 75: 011927
19. Pecora LM, Carroll TL. 1990. Synchronization in chaotic systems. *Physical Review Letters* 64: 821-24
20. Heagy JF, Carroll TL, Pecora LM. 1994. Synchronous chaos in coupled oscillator systems. *Physical Review E* 50: 1874-85
21. Xie Y, Hu G, Sato D, Weiss JN, Garfinkel A, Qu Z. 2007. Dispersion of refractoriness and induction of reentry due to chaos synchronization in a model of cardiac tissue. *Phys. Rev. Lett.* 99: 118101
22. Stanley HE. 1999. Scaling, universality, and renormalization: Three pillars of modern critical phenomena. *Rev. Mod. Phys.* 71: S358-S66
23. Bak P, Tang C, Wiesenfeld K. 1988. Self-organized criticality. *Phys Rev A* 38: 364-74
24. Nivala M, Ko CY, Nivala M, Weiss JN, Qu Z. 2012. Criticality in intracellular calcium signaling in cardiac myocytes. *Biophys J* 102: 2433-42
25. Bak P. 1997. *How Nature Works: The Science of Self-Organized Criticality*. New York: Oxford University Press
26. Nusse HE, Yorke JA. 1996. Basins of Attraction. *Science* 271: 1376-80